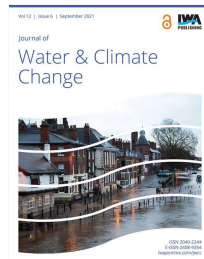


## Volume 12, Issue 6

1 September 2021

[< Previous Article](#)  
[Next Article >](#)  
[Article Contents](#)[Abstract](#)[HIGHLIGHTS](#)[INTRODUCTION](#)[METHODS](#)[RESULTS AND DISCUSSION](#)[CONCLUSIONS](#)[DATA AVAILABILITY  
STATEMENT](#)[REFERENCES](#)

RESEARCH ARTICLE | MAY 18 2021

Drought detection in Java Island based on Standardized Precipitation and Evapotranspiration Index (SPEI) 

Suroso; Dede Nadhilah; Ardiansyah; Edwin Aldrian



Journal of Water and Climate Change (2021) 12 (6): 2734–2752.

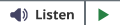
<https://doi.org/10.2166/wcc.2021.022> [Article history](#) [Views](#) ▼ [PDF](#) [Share](#) ▼ [Tools](#) ▼

## Abstract



This study reports a drought analysis which was carried out using the Standardized Precipitation and Evapotranspiration Index (SPEI) to determine the spatial and temporal level of drought risk in Java, Indonesia. Apart from using the SPEI, this study also used the SPI (Standardized Precipitation Index) as a comparison in detecting drought and also validated with historical drought occurrences. Temporal variations of SPI and SPEI values were discussed by considering different timescales (monthly to yearly). Pearson's correlations between both drought indices were calculated to see how similar both indices were. Also, the Kolmogorov–Smirnov tests were used for the similarity test of two kinds of distributions. The results obtained from this analysis showed that the correlation coefficient between the SPI and SPEI models was relatively high on a monthly scale and consistently increased along with the increase of temporal scales but had a decreasing trend during the dry season. However, the SPI detected drought severity with an excessively high estimate in comparison with the SPEI. Greater spatial extents of drought estimation were also generated by SPI followed by SPEI in comparison to factual drought occurrences. As a consequence, SPEI becomes more moderate and SPI as a conservative approach for estimating drought events.

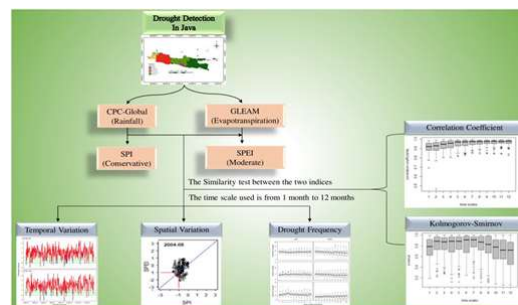
## HIGHLIGHTS



- The drought severity generated by SPI is revealed to be systematically higher than SPEI for most of the given month period.
- In detecting drought, SPI is very conservative, while SPEI is moderate.
- The correlation between SPI and SPEI will be stronger if the timescale used is longer.
- Rainfall is the main cause of the drought, but the existence of evapotranspiration becomes important for a longer timescale.

## Graphical Abstract

## Graphical Abstract

[VIEW LARGE](#)[DOWNLOAD SLIDE](#)**Keywords:** drought, Indonesia, Java Island, SPEI

## INTRODUCTION



Drought is a natural phenomenon that occurs as a result of a high rainfall deficit (Wang & Asefa 2019). This later influences the agricultural sector in Indonesia directly. It was reported by Indonesian Statistics (BPS) that the potential financial loss due to drought in agriculture is

## Editorial Board

### Editor in Chief

#### Prof D. Nagesh Kumar

Department of Civil Engineering,  
Associate Faculty, Centre for Earth Sciences (CEaS),  
Associate Faculty, Interdisciplinary Centre for Water Research (ICWaR),  
Associate Faculty, Divecha Centre for Climate Change (DCCC),  
Indian Institute of Science,  
Bangalore 560 012,  
India  
[E-mail](#)

### Editors

**Sangaralingam Ahilan**, Civil Engineering, University of Exeter, UK  
**Alla Aleksanyan**, Institute of Botany aft. A.L. Takhtajyan NAS RA, and Department of Geobotany and Plant Eco-Physiology, Armenian National Agrarian University, Armenia  
**K.W. Chau**, Department of Civil & Environmental Engineering, The Hong Kong Polytechnic University, Hong Kong  
**Lei Cheng**, Department of Hydrology and Water Resources, School of Water Resources and Hydropower Engineering, Wuhan University, China  
**Nanco Dolman**, Leading Professional in Water Resilient Cities, Royal Haskoning DHV, The Netherlands  
**Ahmed El Kenawy**, Department of Geography, Mansoura University, Egypt  
**Subimal Ghosh**, Civil Engineering, Indian Institute of Technology Bombay, India  
**Gordon Huang**, Environmental Systems Engineering, University of Regina, Canada  
**Kei Ishida**, Centre for Water Cycle, Marine Environment and Disaster Management, Kumamoto University, Japan  
**K. Srinivasa Raju**, Civil Engineering, Birla Institute of Technology and Science Pilani, Hyderabad Campus, India  
**Aavudai Anandhi Swami**, Biological Systems Engineering, Florida A&M University, USA  
**Toan Trinh**, Civil and Environmental Engineering, UC Davis, USA  
**Yueping Xu**, Department of Hydraulic Engineering, College of Civil Engineering, Zhejiang University, China

### International Editorial Board

**Dr Sankar Arumugam**, North Carolina State University, USA  
**Professor Simon Beecham**, University of South Australia, Australia  
**Professor Rutger de Graaf**, Rotterdam University of Applied Sciences, The Netherlands  
**Dr Shaleen Jain**, University of Maine, USA  
**Dr Fiona Johnson**, University of New South Wales, Australia  
**Dr Adam Lovell**, Water Services Association of Australia, Australia  
**Mr Daniel A. Nolasco**, NOLASCO & Assoc. Inc., Argentina  
**Mr Rob Renner**, Water Research Foundation, USA



Issues Select Year 2021 ▾ Issue 1 September - Volume 12, Issue 6, Pages 2147 - 2874 ▾

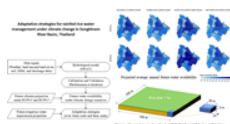
## Issue Navigation

Search within issue:

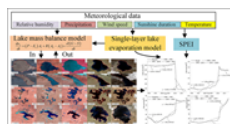
## RESEARCH ARTICLE

**Potential of household photobioreactor for algae cultivation**

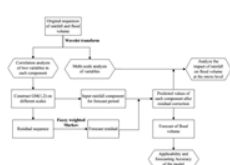
Ashrakat Osama; Hadeel Hosney; M. S. Moussa

[Abstracts](#)[View article](#)[Supplementary data](#)[PDF](#)**Adaptation strategies for rainfed rice water management under climate change in Songkhram River Basin, Thailand**

Siriwat Boonwichai; Sangam Shrestha; Pragya Pradhan; Mukand S. Babel; Avishek Datta

[Abstracts](#)[View article](#)[Supplementary data](#)[PDF](#)**Investigation of dynamic lake changes in Zhuonai Lake-Salt Lake Basin, Hoh Xil, using remote sensing images in response to climate change (1989–2018)**

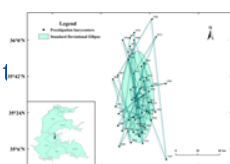
Zukang Hu; Debao Tan; Xiongfei Wen; Beiqing Chen; Dingtao Shen

[Abstracts](#)[View article](#)[PDF](#)**Multi-scale flood prediction based on GM (1,2)-fuzzy weighted Markov and wavelet analysis**

Jinping Zhang; Yuhao Wang; Yong Zhao; Hongyuan Fang

[Abstracts](#)[View article](#)[PDF](#)

Skip 1

**Temporal and spatial distributions of precipitation on the Huang-Huai-Hai Plain during 1960–2019, China**

Minhua Ling; Hongbao Han; Xingling Wei; Cuimei Lv

[Abstracts](#)[View article](#)[PDF](#)

## Impact of climate change on groundwater resource in a region with a fast depletion rate: the Mississippi Embayment

Ying Ouyang; Yongshan Wan; Wei Jin; Theodor D. Leininger; Gary Feng ...

[Abstract](#)
[View article](#)
[PDF](#)


## Autoregressive distributed lag (ARDL) approach to study the impact of climate change and other factors on rice production in South Korea

Muhammad Nasrullah; Muhammad Rizwanullah; Xiuyuan Yu; Hyeonsoo Jo; Muhammad Tayyab Sohail ...

[Abstracts](#)
[View article](#)
[PDF](#)

## Evaluating watershed hydrological responses to climate changes at Hangar Watershed, Ethiopia

Abdata Wakjira Galata; Kiyya Tesfa Tullu; Abebe Chala Guder

[Abstract](#)
[View article](#)
[PDF](#)

## Distribution characteristics, enrichment patterns and health risk assessment of dissolved trace elements in river water in the source region of the Yangtze River

Min Liu; Liangyuan Zhao; Qingyun Li; Yuan Hu; Huawei Huang ...

[Abstract](#)
[View article](#)
[Supplementary data](#)
[PDF](#)

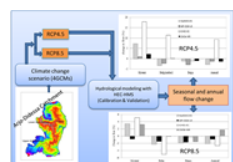

## Redefining the application of an evolutionary algorithm for the optimal pipe sizing problem

Nikita Palod; Vishnu Prasad; Ruchi Khare

[Abstracts](#)
[View article](#)
[Supplementary data](#)
[PDF](#)

## Statistical downscaling using principal component regression for climate change impact assessment at the Cauvery river basin

Parthiban Loganathan; Amit Baburao Mahindrakar

[Abstract](#)
[View article](#)
[Supplementary data](#)
[PDF](#)


## Impact of climate change on the streamflow of the Arjo-Didessa catchment under RCP scenarios

Wudeneh Temesgen Bekele; Alemseged Tamiru Haile; Tom Rientjes

[Abstracts](#)
[View article](#)
[PDF](#)

## Linking climate change to soil loss estimation in the Kosi river basin, India

Aadil Towheed; Thendiyath Roshni

[Skip to Main Content](#)

[Abstract](#)
[View article](#)
[PDF](#)

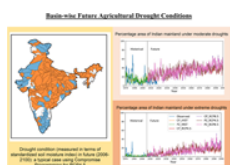
## Application of the HBV model for the future projections of water levels using dynamically downscaled global climate model data

Lia Pervin; Thian Yew Gan; Hester Scheepers; Md Saiful Islam

[Abstract](#)
[View article](#)
[Supplementary data](#)
[PDF](#)

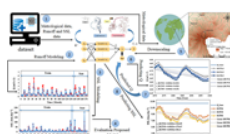
## Spatiotemporal variation characteristics of extreme precipitation in the upper reaches of the Hongshui River Basin during 1959–2016

Ya Huang; Ling Yi; Weihua Xiao; Guibing Hou; Yuyan Zhou

[Abstract](#)
[View article](#)
[PDF](#)


## Assessment of basin-wise future agricultural drought status across India under changing climate

Mayank Suman; Rajib Maity

[Abstracts](#)
[View article](#)
[PDF](#)


## Modeling and predicting suspended sediment load under climate change conditions: a new hybridization strategy

Saeed Farzin; Mahdi Valikhan Anaraki

[Abstracts](#)
[View article](#)
[PDF](#)

## Risk assessment of possible impacts of climate change and irrigation on wheat yield and quality with a modified CERES-Wheat model

Jianchao Liu; Wenbin Yao; Meijun Jiang

[Abstract](#)
[View article](#)
[PDF](#)

## Assessment of combined sewer overflows impacts under flooding in coastal cities

Helieh Abbasi; Amin Zeynolabedin; Gholamreza Nabi Bidhendi

[Abstract](#)
[View article](#)
[Supplementary data](#)
[PDF](#)

## Health-risk assessment for roof-harvested rainwater via QMRA in Ikorodu area, Lagos, Nigeria

Chukwuemeka Kingsley John; Jaan H. Pu; Rodrigo Moruzzi; Manish Pandey

[Abstract](#)
[View article](#)
[Supplementary data](#)
[PDF](#)

## Hydrological simulation of the Jialing River Basin using the MIKE SHE model in changing climate

Jing Zhang; Meng Zhang; Yongyu Song; Yuequn Lai

[Abstract](#)
[View article](#)
[PDF](#)

## Potential soil moisture deficit: A useful approach to save water with enhanced growth and productivity of wheat crop

[Skip to Main Content](#)

Shahbaz Khan; Atif Rasool; Sohail Irshad; Muhammad Bilal Hafeez; Madad Ali ...

[Abstract](#)
[View article](#)
[Supplementary data](#)
[PDF](#)

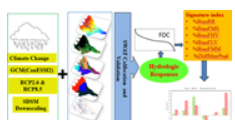
## Quantifying the potential impacts of land-use and climate change on hydropower reliability of Muzizi hydropower plant, Uganda

Hilary Keneth Bahati; Abraham Ogenrwoth; Jotham Ivan Sempewo

[Abstract](#)
[View article](#)
[Supplementary data](#)
[PDF](#)


## Long-term water-energy demand prediction using a regression model: a case study of Addis Ababa city

Bedassa Dessalegn Kitessa; Semu Moges Ayalew; Geremew Sahilu Gebrie; Solomon Tesfamariam Teferi

[Abstracts](#)
[View article](#)
[PDF](#)


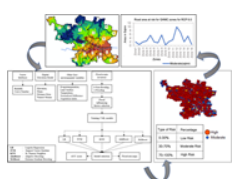
## Assessing watershed hydrological response to climate change based on signature indices

Atiyeh Fatehifar; Mohammad Reza Goodarzi; Seyedeh Sima Montazeri Hedesh; Parnian Siahvashi Dastjerdi

[Abstracts](#)
[View article](#)
[PDF](#)

## Changes in length of rainy season and rainfall extremes under moderate greenhouse gas emission scenario in the Veia catchment, Ghana

Isaac Larbi; Bessah Enoch; Clement Nyamekye; Joshua Amuzu; Gloria C. Okafor ...

[Abstract](#)
[View article](#)
[PDF](#)


## Application of machine learning algorithms for flood susceptibility assessment and risk management

R. Madhuri; S. Sistla; K. Srinivasa Raju

[Abstracts](#)
[View article](#)
[Supplementary data](#)
[PDF](#)

## Detection and attribution of reference evapotranspiration change (1951–2020) in the Upper Yangtze River Basin of China

Manlin Wang; Yu Zhang; Yan Lu; Xulong Gong; Li Gao

[Abstract](#)
[View article](#)
[PDF](#)

## The construction of the flow duration curve and the regionalization parameters analysis in the northwest of China

Jinkai Luan; Dengfeng Liu; Mu Lin; Qiang Huang

[Abstract](#)
[View article](#)
[PDF](#)

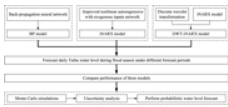
## Effect of local calibration on the performance of the Hargreaves reference crop evapotranspiration equation

S. Niranjani; Lakshman Nandagiri

[Abstract](#)
[View article](#)
[PDF](#)

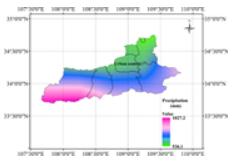
[Skip to Main Content](#)

## Flood forecasting using an improved NARX network based on wavelet analysis coupled with uncertainty analysis by Monte Carlo simulations: a case study of Taihu Basin, China



Feiqing Jiang; Zengchuan Dong; Zeng'an Wang; Yiqing Zhu; Moyang Liu ...

[Abstracts](#) [View article](#) [PDF](#)



**Spatial and temporal variation of precipitation characteristics in the semiarid region of Xi'an, northwest China**

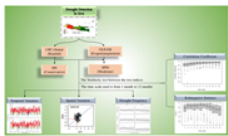
Hao Han; Jingming Hou; Rengui Jiang; Jiahui Gong; Ganggang Bai ...

[Abstracts](#) [View article](#) [PDF](#)

**Estimating surface water and vadose water resources for an ungauged inland catchment in Vietnam**

Liem Duy Nguyen; Phuong Dong Nguyen Dang; Loi Kim Nguyen

[Abstract](#) [View article](#) [Supplementary data](#) [PDF](#)



**Drought detection in Java Island based on Standardized Precipitation and Evapotranspiration Index (SPEI)**

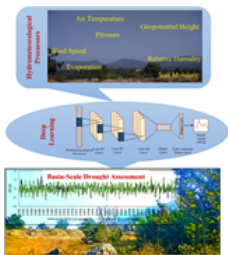
Suroso; Dede Nadhilah; Ardiansyah; Edvin Aldrian

[Abstracts](#) [View article](#) [PDF](#)

**Assessment of temporal change in the tails of probability distribution of daily precipitation over India due to climatic shift in the 1970s**

Neha Gupta; Sagar Rohidas Chavan

[Abstract](#) [View article](#) [Supplementary data](#) [PDF](#)



**Potential of Deep Learning in drought assessment by extracting information from hydrometeorological precursors**

Rajib Maity; Mohd Imran Khan; Subharthi Sarkar; Riya Dutta; Subhra Sekhar Maity ...

[Abstracts](#) [View article](#) [PDF](#)

**Effect of de-trending climatic parameters on temporal changes of reference evapotranspiration in the eastern Himalayan region of Sikkim, India**

Vanita Pandey; Indira Taloh; P. K. Pandey

[Abstract](#) [View article](#) [PDF](#)

**Investigation of artificial neural network performance in the aerosol properties retrieval**

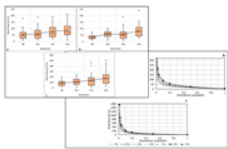
Nishi Srivastava; D. Vignesh; Nisheeth Saxena

[Abstract](#) [View article](#) [PDF](#)

[Skip to Main Content](#)

**Quantitative analysis of the impacts of climate and land-cover changes on urban flood runoffs: a case of Dar es Salaam, Tanzania**

Philip Mzava; Patrick Valimba; Joel Nobert



Abstracts

View article

PDF

Identifying most promising agronomic adaptation strategies to close rainfed rice yield gap in future: a model-based assessment

Subhankar Debnath; Ashok Mishra; D. R. Mailapalli; N. S. Raghuwanshi

Abstract

View article

PDF

Cover Image

Front Matter

Table of Contents

Back Matter

Editorial Board

All Issues

Email alerts

Latest Articles

New issue alert

Latest	Most Read	Most Cited
Regional modeling of winter wheat yield and water productivity under water-saving irrigation scenarios		
The key role for groundwater in urban water-supply security		
Prediction of future groundwater levels under representative concentration pathway scenarios using an inclusive multiple model coupled with artificial neural networks		
Rainfall extremes under climate change in the Pasak River Basin, Thailand		
Numerical modelling of breaking wave impact loads on a vertical seawall retrofitted with different geometrical configurations of recurve parapets		

Journal of  
Water & Climate Change

ISSN 2040-2244 EISSN 2408-9354

Skip to Main Content

[Journals](#)

[Contact us](#)

[eBooks](#)

[Sign Up for Our Mailing List](#)

[Open Access](#)

[Collections](#)

**IWA Publishing**

Republic – Export Building, Units 1.04 & 1.05

1 Clove Crescent

London, E14 2BA, UK

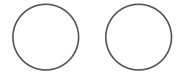
[IWAPublishing.com](http://IWAPublishing.com)

[IWA-network.org](http://IWA-network.org)

[IWA-connect.org](http://IWA-connect.org)

**Telephone:** +44 207 654 5500

**Fax:** +44 207 654 5555



[Cookie Policy](#)

[Terms & Conditions](#)

[Privacy](#)

[Site Map](#)

[Get Adobe Acrobat Reader](#)

©Copyright 2021 IWA Publishing

# Journal of Water and Climate Change

COUNTRY

[United Kingdom](#)

 Universities and research institutions in United Kingdom

SUBJECT AREA AND CATEGORY

[Earth and Planetary Sciences](#)  
[Atmospheric Science](#)

[Environmental Science](#)  
[Global and Planetary Change](#)  
[Management, Monitoring, Policy and Law](#)  
[Water Science and Technology](#)

PUBLISHER

[IWA Publishing](#)

H-INDEX

25

PUBLICATION TYPE

[Journals](#)

ISSN

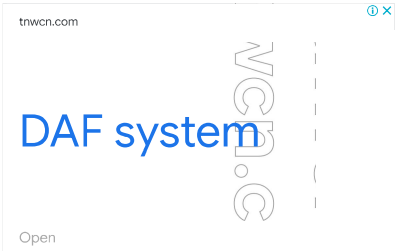
20402244

COVERAGE

2010-2021

INFORMATION

[Homepage](#)  
[How to publish in this journal](#)  
[Contact](#)



SCOPE

Journal of Water and Climate Change publishes novel peer-reviewed research and practitioner papers on all aspects of water science, technology, management and innovation in response to climate change, with emphasis on reduction of energy usage. Review papers are particularly encouraged. The journal's scope includes but is not limited to articles relating climate change to: Energy reduction technologies and strategies Hydrology Extreme events (floods, rainstorms, droughts) Energy and nutrient recovery in wastewater treatment Agricultural water use and climate change Water resource management including accounting, water reuse and demand management Technologies for reducing greenhouse emissions for water and wastewater treatment Carbon accounting in the water sector Targets and strategies for carbon emissions reduction Policy and practice of adaptation and mitigation of climate change in the water sector Predictive modelling of water resources Waterborne disease Inland and coastal waters, including both surface and ground waters

 Join the conversation about this journal

## DAF For Wastewater

can effectively remove the suspended matter, grease, rubber substa  
the sewage

tnwcn.com



# DAF For Wastewater

can effectively remove the suspended matter, grease, rubber substa  
the sewage

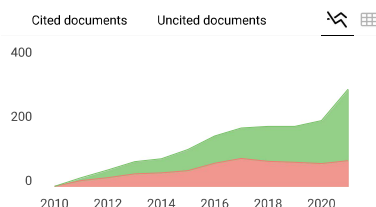
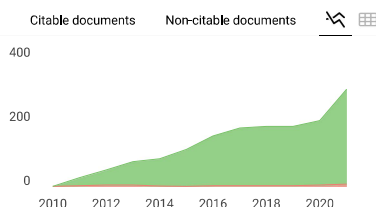
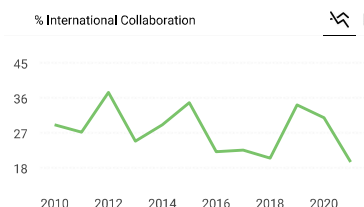
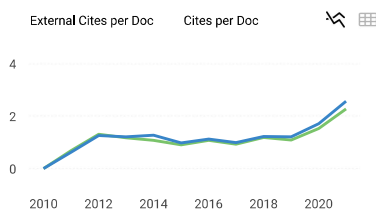
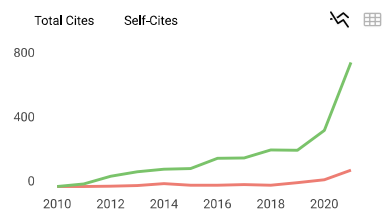
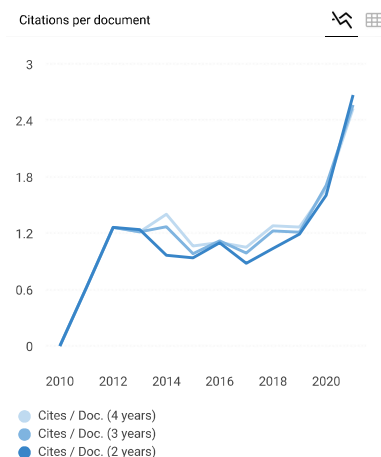
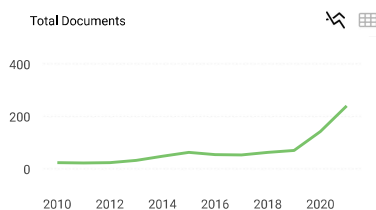
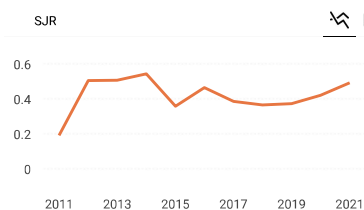
trwcn.com

0

## FIND SIMILAR JOURNALS ?

options

1 <b>Hydrology</b> CHE  <b>74%</b> similarity	2 <b>Journal of Hydrology: Regional Studies</b> NLD  <b>72%</b> similarity	3 <b>Revista Brasileira de Recursos Hidricos</b> BRA  <b>66%</b> similarity	4 <b>International Journal of Water</b> GBR  <b>64%</b> similarity	5 <b>International Journal of Hydrology Science and</b> GBR  <b>64%</b> similarity
--	---	--	---	---



**Journal of Water and Climate Change**

**Q2**

Management, Monitoring, Policy and Law

best quartile

**SJR 2021**

**0.49**

powered by scimagojr.com

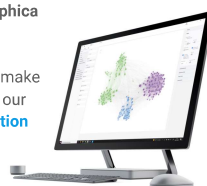
← Show this widget in your own website

Just copy the code below and paste within your html code:

<a href="https://www.scimag

## SCImago Graphica

Explore, visually communicate and make sense of data with our **new data visualization tool**.



Metrics based on Scopus® data as of April 2022

hello

reply

W **Wa kouakou charles N'DRI** 4 years ago

Hello,

I am a doctoral student at the end of the thesis cycle. I am therefore in the process of defense and it is important that I make publications. Indeed, I am very happy to have been recommended by my teachers for this review, which in my opinion is very interesting and whose scope takes into account the main lines of my article. I will be very grateful to have my article published in your magazine.

reply

#### Leave a comment

Name

Email

(will not be published)

☐ I'm not a robot

reCAPTCHA  
Privacy • Terms

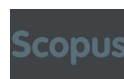
Submit

The users of Scimago Journal & Country Rank have the possibility to dialogue through comments linked to a specific journal. The purpose is to have a forum in which general doubts about the processes of publication in the journal, experiences and other issues derived from the publication of papers are resolved. For topics on particular articles, maintain the dialogue through the usual channels with your editor.

Developed by:



Powered by:



Follow us on @ScimagoJR

Scimago Lab, Copyright 2007-2022. Data Source: Scopus®

EST MODUS IN REBUS  
Horatio (Satire 1.1.105)

[Edit Cookie Consent](#)



# Source details

Feedback >

Compare sources >

## Journal of Water and Climate Change

Open Access

Scopus coverage years: from 2010 to 2022

Publisher: IWA Publishing

ISSN: 2040-2244

Subject area: 

Environmental Science: Management, Monitoring, Policy and Law

Environmental Science: Water Science and Technology

Environmental Science: Global and Planetary Change

Earth and Planetary Sciences: Atmospheric Science

Source type: Journal

View all documents >

Set document alert

Save to source list

CiteScore 2021	<div></div>
2.6	
SJR 2021	<div></div>
0.492	
SNIP 2021	<div></div>
0.778	

CiteScore

CiteScore rank & trend

Scopus content coverage

i

Improved CiteScore methodology

CiteScore 2021 counts the citations received in 2018-2021 to articles, reviews, conference papers, book chapters and data papers published in 2018-2021, and divides this by the number of publications published in 2018-2021. [Learn more >](#)

x

CiteScore

2021

2.6

=

1,329 Citations 2018 - 2021

506 Documents 2018 - 2021

Calculated on 05 May, 2022

CiteScoreTracker 2022

3.8

=

2,557 Citations to date

672 Documents to date

Last updated on 05 January, 2023 • Updated monthly

### CiteScore rank 2021

Category	Rank	Percentile
Environmental Science Management, Monitoring, Policy and Law	#183/376	51st
Environmental Science Water Science and Technology	#129/237	45th
Environmental Science Global and Planetary Change	#62/109	43rd

View CiteScore methodology >

CiteScore FAQ >

Add CiteScore to your site

## About Scopus

- What is Scopus
- Content coverage
- Scopus blog
- Scopus API
- Privacy matters

## Language

- 日本語版を表示する
- 查看简体中文版本
- 查看繁體中文版本
- Просмотр версии на русском языке

## Customer Service

- Help
- Tutorials
- Contact us

# Drought detection in Java Island based on Standardized Precipitation and Evapotranspiration Index (SPEI)

Suroso, Dede Nadhilah, Ardiansyah and Edvin Aldrian

## ABSTRACT

This study reports a drought analysis which was carried out using the Standardized Precipitation and Evapotranspiration Index (SPEI) to determine the spatial and temporal level of drought risk in Java, Indonesia. Apart from using the SPEI, this study also used the SPI (Standardized Precipitation Index) as a comparison in detecting drought and also validated with historical drought occurrences. Temporal variations of SPI and SPEI values were discussed by considering different timescales (monthly to yearly). Pearson's correlations between both drought indices were calculated to see how similar both indices were. Also, the Kolmogorov–Smirnov tests were used for the similarity test of two kinds of distributions. The results obtained from this analysis showed that the correlation coefficient between the SPI and SPEI models was relatively high on a monthly scale and consistently increased along with the increase of temporal scales but had a decreasing trend during the dry season. However, the SPI detected drought severity with an excessively high estimate in comparison with the SPEI. Greater spatial extents of drought estimation were also generated by SPI followed by SPEI in comparison to factual drought occurrences. As a consequence, SPEI becomes more moderate and SPI as a conservative approach for estimating drought events.

**Key words** | drought, Indonesia, Java Island, SPEI

**Suroso** (corresponding author)

**Dede Nadhilah**

Department of Civil Engineering, Faculty of Engineering,  
Jenderal Soedirman University,  
Purwokerto,  
Indonesia  
E-mail: [surosotsipil@unsoed.ac.id](mailto:surosotsipil@unsoed.ac.id)

**Ardiansyah**

Department of Agricultural Engineering, Faculty of Agricultural,  
Jenderal Soedirman University,  
Purwokerto,  
Indonesia

**Edvin Aldrian**

Agency for the Assessment and Application of Technology (BPPT),  
Jakarta,  
Indonesia

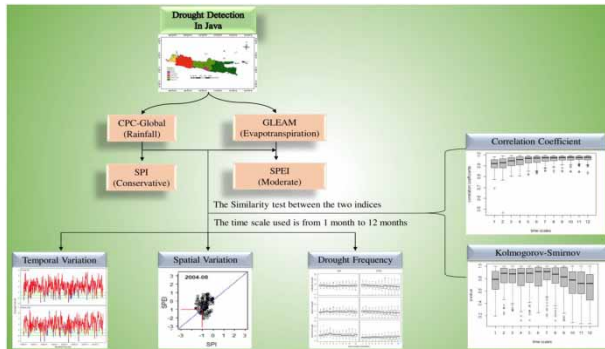
## HIGHLIGHTS

- The drought severity generated by SPI is revealed to be systematically higher than SPEI for most of the given month period.
- In detecting drought, SPI is very conservative, while SPEI is moderate.
- The correlation between SPI and SPEI will be stronger if the timescale used is longer.
- Rainfall is the main cause of the drought, but the existence of evapotranspiration becomes important for a longer timescale.

This is an Open Access article distributed under the terms of the Creative Commons Attribution Licence (CC BY 4.0), which permits copying, adaptation and redistribution, provided the original work is properly cited (<http://creativecommons.org/licenses/by/4.0/>).

doi: 10.2166/wcc.2021.022

## GRAPHICAL ABSTRACT



## INTRODUCTION

Drought is a natural phenomenon that occurs as a result of a high rainfall deficit (Wang & Asefa 2019). This later influences the agricultural sector in Indonesia directly. It was reported by Indonesian Statistics (BPS) that the potential financial loss due to drought in agriculture is estimated at three trillion rupiahs per year (BPS 2019). Additionally, beside having a direct impact on decreasing food productivity, drought can also have indirect environmental impacts, such as forest fires (Holden *et al.* 2019).

According to data from the Ministry of Environment and Forestry, the total number of forest fires in 2019 reached 1,649,258 hectares, a significant increase from the total of forest fires in 2018 of 529,266 hectares. In September 2019, it was reported by the National Disaster Management Agency (BNPB) that more than 900,000 people experienced respiratory problems due to smoke resulting from forest fires (World Bank 2019). Meanwhile, throughout 2019, Indonesia's total losses due to forest and land fires reached US\$ 5.2 million (Rp. 72.95 trillion), which was equivalent to 0.5% of Indonesia's Gross Domestic Product (GDP) (World Bank 2019). Next, based on water availability data in 2019 compiled by the Research and Development Center for Water Resources of the Ministry of Public Works and Public Housing (PUPR), the availability rate of water for one person in Java Island is 1,169 m<sup>3</sup>/year and will continue to decline until 2040 when the availability rate of water for

one person is limited to 476 m<sup>3</sup>/year, which is categorized as severe scarcity. Having the potential to cause severe impacts, drought has become a disaster that has received serious attention at both national and international levels, since it greatly affects people's activities in various sectors of life (Stampfli *et al.* 2018).

Drought that occurs slowly (called slow on-set drought) may have a severe long-term impact on various sectors of human life that needs to be anticipated. Therefore, mitigation efforts are needed to reduce any potential impacts of drought (Gebremeskel *et al.* 2019). One of the non-structural mitigation strategies that can be conducted is implementing early detection systems to monitor drought by creating a disaster risk distribution map. Disaster risk mapping is a starting point for raising public awareness, informing policy-makers or authorities to encourage disaster management (Blauhut 2020).

In an early detection system, understanding the characteristics of drought is imperative. By identifying and representing drought characteristics and indicators, a drought index or a combination of drought indices is usually used (Blauhut 2020). A drought index consists of several drought indicators that can explain quantitatively the intensity, duration, and severity of drought (Wang & Asefa 2019). Drought events can be analysed because several drought indices have been developed to detect and monitor drought

events (Wang *et al.* 2019). Two drought indices that are often used for drought analysis are the Standardized Precipitation Index (SPI) and the Standardized Precipitation and Evapotranspiration Index (SPEI).

SPI is a drought index that has been standardized to measure rainfall anomalies and is the main indicator of drought recommended by the World Meteorological Organization (Stagge *et al.* 2015). The precipitation data used in this research is obtained from Global Precipitation, which has the advantage of providing precipitation data for a long time period from 1979 to 2020. The data are available almost in real-time for a whole continent so that the quality of the data is confirmed to be very good, in terms of both spatial and temporal coverages. The study location focuses on Java Island because according to the data compiled by the meteorological, climatological, and geophysical agency (BMKG), Java Island has been the island with the highest frequency of being hit by drought compared with the other islands in Indonesia for 30 years from 1979 to 2009 and is still prone to experiencing drought until now.

Beside that, the utilization of SPI and SPEI as the drought indices in this study is because these two indices are most often used, especially SPI as the main parameter in monitoring drought in Indonesia by the BMKG. The use of SPI as a comparison index is due to the existence of the same parameter as SPEI in analysing drought, namely precipitation. Additionally, apart from SPI and SPEI, there are various types of drought indices that are developed to suit the conditions of certain areas. One of them is the Hurst index, which is developed to determine annual and seasonal trends with hydrological and climatic variables in streamflow (Shahid & Rahman 2020).

The paper is divided into four sections, namely Introduction, Methods, Results and discussion, and Conclusions. The first section describes the introduction of why this study is essential to conduct, the study location, and data available. Then, the methods of SPEI and SPI approaches as well as drought classification are explained in the section 'Methods'. Some research findings, such as behaviours of SPI and SPEI methods, for detecting droughts in terms of temporal and spatial characteristics are discussed in the section 'Results and discussion'. Finally, in the section 'Conclusions', the conclusion gives a brief summary of the findings and their implications.

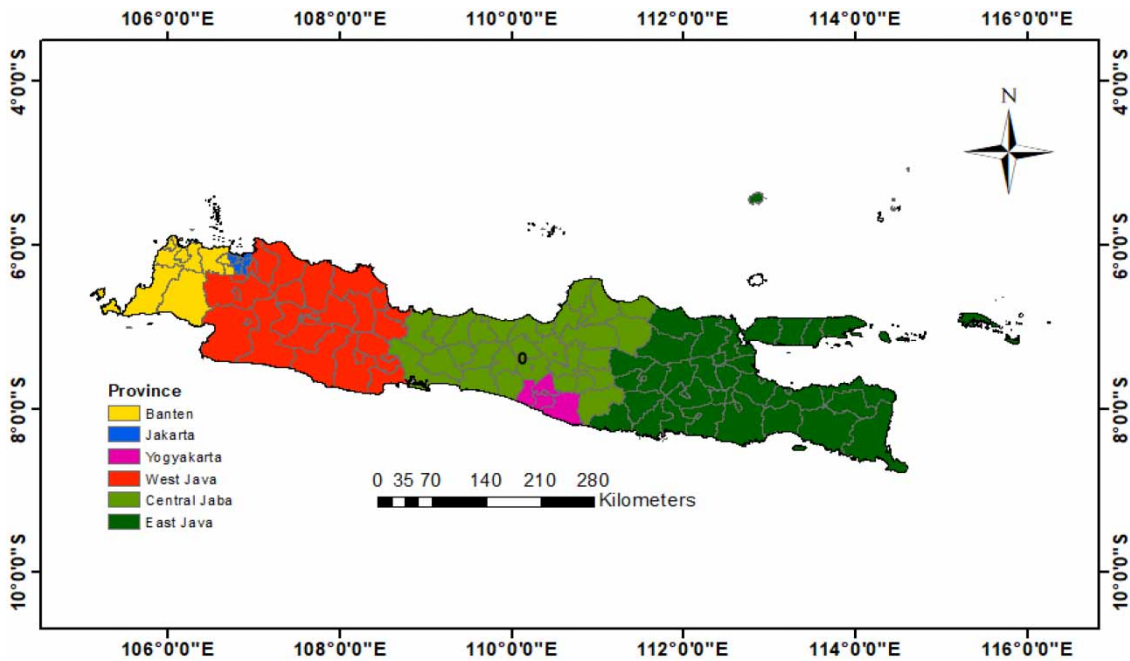
## Study location

The study location was Java Island, which is situated between 113°48'10" to 113°48'26" East Longitude and 7°50'10" to 7°56'41" South Latitude as shown in Figure 1. Java Island has a total area of 138,793 km<sup>2</sup> with a length from east to west of 1,033 km, and within its central position, it has a width of about 104 km, while in the western part, the width is about 98 km and the eastern part is about 107 km. Administratively, Java Island consists of six provinces: four provinces include Banten with the provincial capital of Serang, West Java with the provincial capital of Bandung, Central Java with the provincial capital of Semarang, and East Java with the provincial capital of Surabaya; two special areas at the provincial level, namely Jakarta and Yogyakarta. Furthermore, Banten province consists of six districts/cities, Jakarta province consists of five municipalities, West Java province consists of 25 districts/cities, Central Java province consists of 35 districts/cities, Yogyakarta province consists of five districts/cities, and East Java province consists of 38 districts/cities.

Java Island has an annual average temperature of 22°–29 °C, and usually during the day and the dry season, the temperature in the coastal area can reach up to 34 °C, while the average humidity is around 75%. Meanwhile, the annual rainfall ranges from 1,773 to 3,710 mm. Based on the distribution of average monthly rainfall, Java Island has a monsoon type that makes it experience only two seasons, namely the dry season that occurs from April to September (dry months) and the rainy season that occurs from October to March (wet months).

## Drought historical data

To anticipate the occurrence of drought, future projections could be carried out to determine the recurring drought period by utilizing historical data. Drought historical data are recorded data from reports of previous droughts that have occurred in a certain time period. Drought historical data of Java were obtained through the Indonesian Disaster Information Data (DIBI) recorded by the National Disaster Management Agency (BNPB), and the available data taken were from 2003 to 2019. These data contained coordinates

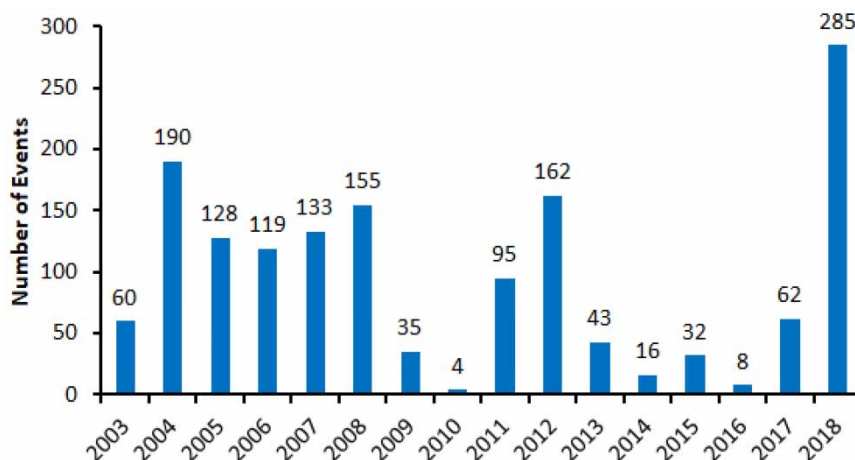


**Figure 1** | Map of Java Island.

of the location, name of the district/city and province, number of victims (injured, died, evacuated, and missing), material losses, and a description of the events that were recorded directly at the disaster site. Drought historical data would be used for validation coupled with the results of the SPI and SPEI analyses to identify a correlation between the two. As for the total data on drought events in Java Island, it is illustrated by [Figure 2](#).

### Precipitation data

In this research, precipitation data were obtained from Global Daily Precipitation (CPC-Global). CPC-Global was developed by the National Oceanic and Atmospheric Administration (NOAA), which is the first product of the CPC Unified Precipitation Project ([Sun et al. 2018](#)). This project is devoted to creating an integrated set of precipitation



**Figure 2** | Total event of drought in Java Island.

products that have consistent quantity and improved quality using the optimal interpolation objective analysis technique by combining all available sources of information in the CPC-Global (Sun *et al.* 2018). CPC-Global has been constructed over the global land areas, with the gauge reports from over 30,000 stations collected from multiple sources, including GTS (Global Telecommunication System), COOP (Cooperative Observer Network), and other national meteorological agencies (Sun *et al.* 2018).

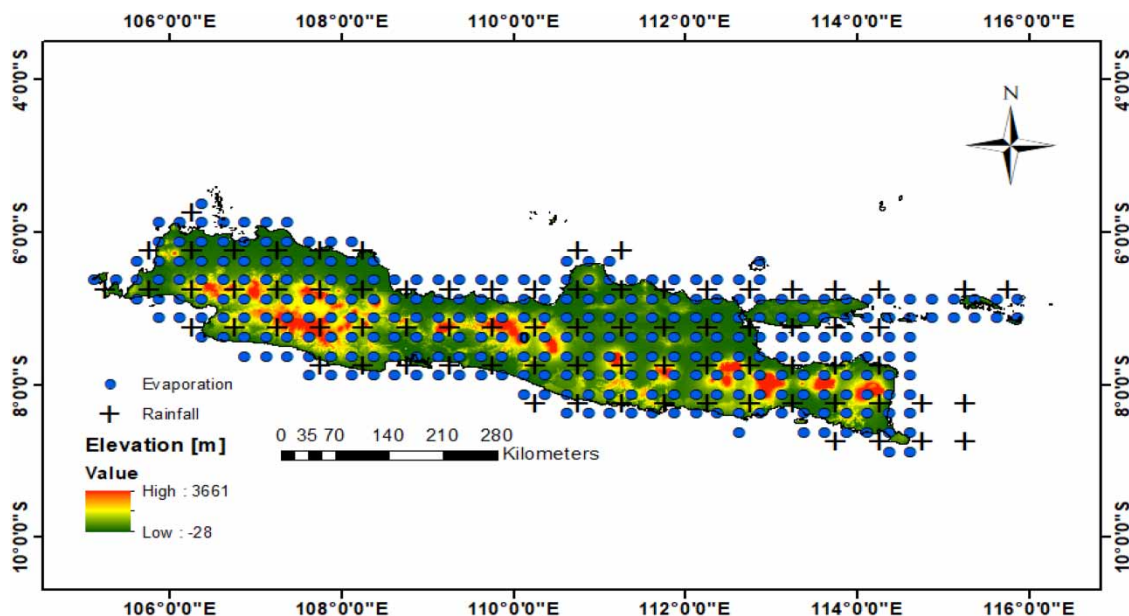
The use of precipitation data from CPC-Global has been widely used for various types of research, especially for predicting hydrological variability and water balance. CPC-Global is used to simulate river flow variability on daily and monthly timescales in the watershed (Shawul & Chakma 2020), a simulation to estimate the effective hydrological processes in the watershed (Pang *et al.* 2020). Even CPC-Global is recommended as precipitation data for use in extreme drought analysis, future climate analysis, and hydrological modelling (Pang *et al.* 2020) and can be useful as a source of precipitation data for hydrological modelling in the tropical regions, where precipitation data are scarce (Shawul & Chakma 2020).

Furthermore, CPC-Global is able to provide daily precipitation data, while in drought analysis, the timescale used is

monthly. Therefore, the daily precipitation data would be accumulated into monthly data. To analyse drought based on SPEI, the form of data used is usually that which comprises more than 40 years, and the data from CPC-Global have fulfilled the requirement in this regard. In contrast to data from satellites such as Tropical Rainfall Measuring Mission (TRMM) (Jati *et al.* 2019; Umiati *et al.* 2019) which only provides data for about 20 years, the quality of Global Precipitation data is said to be better and more reliable. Moreover, the data from CPC-Global have a grid resolution of  $0.5^\circ \times 0.5^\circ$ . Since the grid size for precipitation is different from the evaporation grid size ( $0.25^\circ \times 0.25^\circ$ ), the precipitation grid size was converted into the evaporation grid size first. The following illustration is the image for the precipitation and evaporation data grids (Figure 3).

### Evaporation data

Apart from precipitation, evaporation is an integral component that is used to detect changes in the hydrological cycle and estimate the impact of climate change on water resources (Ghorbani *et al.* 2018). In this research, the evaporation data were obtained from GLEAM (Global Land-surface Evaporation: the Amsterdam Methodology).



**Figure 3** | The investigation location: Java Island, Indonesia. Black plus signs represent precipitation grid points. Blue dots represent evaporation grid points. Please refer to the online version of this paper to see this figure in colour: [doi:10.2166/wcc.2021.022](https://doi.org/10.2166/wcc.2021.022).

GLEAM data sets have already been comprehensively validated against an extensive set of *in situ* observations. A global validation using a large database of *in situ* measurements of evaporation had been conducted from 91 eddy covariance towers (FLUXNET observations). Moreover, soil moisture measurements from 2,325 *in situ* sensors from the database of the International Soil Moisture Network (ISMN) had been taken for further validation.

The GLEAM data sets have also been evaluated over continental Australia (south of Java Island), where they generally perform better (Martens *et al.* 2016, 2017). Especially, GLEAM data have been applied in several regions/countries such as in Africa (Peng *et al.* 2020) and Australia (Martens *et al.* 2016), which are used for multiple hydro-meteorological applications such as to anticipate the availability of water and food due to drought (Peng *et al.* 2020) and for modelling the land water availability on terrestrial evaporation fields (Martens *et al.* 2016). Hence, the evaporation data sets derived from the GLEAM are reasonably used for further analysis in this study.

GLEAM continues to improve its performance in providing data both temporally and spatially; even now there is GLEAM version 3 available. GLEAM v3.3a is a global dataset of land-surface evaporation and root zone soil moisture. The dataset is generated using the Priestley–Taylor equation based on reanalysis surface radiation (ERA-5) and near-surface air temperature (ERA-5), a combination of gauge-based, reanalysis, and satellite-based precipitation (MSWEP v2.2) and satellite-based vegetation optical depth (land parameter retrieval model – LPRM) (Martens *et al.* 2017). GLEAM 3.3a data were selected for this study because this model provided the most complete dataset in terms of spatial extents ( $0.25^\circ \times 0.25^\circ$ ) and continuous temporal coverages (daily) for 39 years (1980–2018). And it provided daily evaporation data, while in a drought analysis, the time-scale used is monthly. Therefore, the daily evaporation data would need to be accumulated first into monthly data.

## METHODS

### SPI development

SPI is a drought index developed by McKee *et al.* (1993) and is one of the most frequently used indices in

drought analysis. SPI is considered to be the simplest index to analyse because it only uses one indicator of drought, namely precipitation, and has a small amount of data in the calculation (Shamshirband *et al.* 2020). Drought analysis with SPI is completed by adding up the rainfall during  $k$  months, then the accumulated rainfall is standardized into a parametric statistical distribution, of which probabilities are converted to the standard normal distribution (McKee *et al.* 1993; Stagge *et al.* 2015). By then, the SPI value can be interpreted statistically, which represents the number of standard deviations from the spatial and temporal accumulated rainfall of the year (Stagge *et al.* 2015).

However, for certain times such as the dry season or summer where the rate of rainfall is minimum, the possibility of rainfall accumulation does not exist (zero precipitation), especially for short periods that occur in between 1 and 3 months. In previous SPI studies that have been reviewed by Stagge *et al.* (2015), to solve the zero precipitation, the SPI value is set based on the historical occurrence (%) of periods with zero precipitation in the following equation:

$$p_{(x)} = p_o + (1 - p_o)F(x_{p>0}, \lambda) \quad (1)$$

where  $p$  represents the probability distributions for accumulated precipitation,  $F(x, \lambda)$  is the parametric univariate distribution functions, and  $x, p_o$  is the historical ratio of periods with zero precipitation.

Nonetheless, this method causes a problem because it provides the maximum SPI value. The average SPI value in the normal distribution should be 0; meanwhile, the value is in between two conditions, 50% is in wet conditions and the other 50% is in dry conditions. In this method, the average SPI value has increased so that the value is above 0 (Stagge *et al.* 2015). Therefore, Stagge *et al.* (2015) in their study provided a solution by making the SPI value maintained for statistical interpretability to be in the condition of zero precipitation based on the ‘center of mass’. By using zero precipitation based on the ‘center of mass’, the average SPI value will always be 0 and will not be skewed under different conditions (dry or wet). The formula used to calculate the probability of

'center of mass' for zero precipitation is shown in the following equation:

$$p_{(x)} = \begin{cases} p_{(x)} = p_o + (1 - p_o)F(x_{p>0}, \lambda), & x > 0 \\ \frac{n_{p=0} + 1}{2(n + 1)}, & x = 0 \end{cases} \quad (2)$$

where  $n$  is the total number of samples in the reference period,  $p$  and  $F(x, \lambda)$  are the probability distribution and the parametric univariate distribution functions for samples that match parameter  $\lambda$  with detectable precipitation accumulation.

After all the probability value has been calculated, the distribution of the SPI value can then be computed. The SPI values require selecting an appropriate parametric probability distribution to convert climate water balance accumulation into standard normal distribution. The selection of an incorrect distribution can cause a fairly high bias in the index value, which results in the value being inaccurate (Stagge *et al.* 2015; Monish & Rehana 2020). The distributions for SPI include normal, log-normal, logistics, log-logistics, Gamma, Gumbel, and Weibull. With extensive statistical testing and relative comparisons such as Kolmogorov–Smirnov (KS), Anderson–Darling (AD), and Shapiro–Wilk, Stagge *et al.* (2015) recommend the gamma distribution to be used for calculating the SPI. The percentage of rejection of the gamma distribution from the results of these tests is the lowest (near to 5%) compared with other distributions so that the gamma distribution becomes the most suitable distribution model. The SPI value with the gamma distribution can be calculated using the following equation:

$$f(x) = \frac{1}{\alpha^\beta \Gamma(\beta)} x^{\beta-1} e^{-\frac{x}{\alpha}}, \quad x > 0 \quad (3)$$

where

$$\Gamma(c) = \int_0^\infty e^{-x} x^{c-1} dx \quad (4)$$

## SPEI development

Different from the SPI analysis, the SPEI analysis is based on the accumulation for  $k$  months and employs the value of the reduction of rainfall with potential evapotranspiration (PET) (Stagge *et al.* 2015). After the accumulation of rainfall minus evapotranspiration is converted into probability, it is then converted into a standard normal distribution to determine the final drought index value. Furthermore, the probability distribution for SPEI requires a location parameter because the climate water balance is not limited by a zero value and can still be analysed, even though the value is negative when the PET value is greater than rainfall. The distributions for SPEI include normal, general logistics, generalized extreme value (GEV), and Pearson Type III distribution (Stagge *et al.* 2015). Stagge *et al.* (2015) suggest to use the GEV distribution when calculating the SPEI after doing some statistical testing such as KS, AD, and Shapiro–Wilk. The suggestion is given because the percentage of rejection of the GEV distribution is the lowest compared with other distributions from the results of these tests so that the GEV distribution becomes the most suitable distribution model, especially for uncertain climatic conditions.

To develop a drought index based on SPEI, it is necessary to ensure that the quality of the precipitation and evaporation data use is complete. SPEI uses the difference between monthly precipitation and PET. After PET is obtained, then the climate water balance for the  $i$ th month ( $D_i$ ) can be calculated by reducing the value of precipitation for the  $i$ th month ( $P_i$ ) with evaporation potential for the  $i$ th month ( $PET_i$ ) as in the following equation:

$$D_i = P_i - PET_i \quad (5)$$

SPEI is standardization based on the GEV distribution. With the GEV distribution, the observed variable will be limited to observing only the maximum or minimum value, which is independent and identically distributed. The probability density function  $f(x)$  of the GEV distribution

is shown in the following equation:

$$f_{(x)} = \begin{cases} \left(\frac{1}{\sigma}\right) \left[ (1 + \xi z_{(x)})^{-\frac{1}{\xi}} \right]^{\xi+1} e^{-\left[ (1 + \xi z_{(x)})^{-\frac{1}{\xi}} \right]}, & \xi \neq 0, 1 + \xi z_{(x)} > 0 \\ \left(\frac{1}{\sigma}\right) e^{-z_{(x)} - e^{-z_{(x)}}} & \xi = 0, -\infty < x < \infty \end{cases} \quad (6)$$

where

$$Z_{(x)} = \frac{x - \mu}{\sigma} \quad (7)$$

$\mu$ ,  $\sigma$ , and  $\xi$  are parameters of location, scale, and shape, respectively, that have been estimated using the maximum probability. The cumulative GEV distribution function  $F(x)$  can be calculated in the following equation:

$$F_{(x)} = e^{-t_{(x)}} \quad (8)$$

where

$$t_{(x)} = \begin{cases} \left( 1 + \xi \left( \frac{x - \mu}{\sigma} \right) \right)^{-\frac{1}{\xi}}, & \xi \neq 0 \\ e^{-(x - \mu)/\sigma}, & \xi = 0 \end{cases} \quad (9)$$

## Drought classification

The drought index is the main variable for assessing the effects of drought and for determining variations in drought characteristics such as duration, intensity, and severity. In this study, the drought analysis will be calculated on a different scale from 1 to 12 months. Based on SPEI calculations as suggested in [McKee et al. \(1993\)](#), drought can be classified into seven categories as listed in [Table 1](#).

SPEI is a standardized variable, and it can be compared with other SPEI values over time and space. Drought occurs when the SPEI value is consistently negative and reaches drought intensity with an SPEI value of  $-1$  or less, and the drought will end if the SPEI value becomes positive. Drought can also be classified based on the frequency of occurrence according to [WMO \(2012\)](#), drought is divided into four categories as listed in [Table 2](#).

**Table 1** | Drought classification based on SPEI value ([McKee et al. 1993](#))

SPEI value	Condition	Class
$\geq 2$	Extremely wet	1
1.5 s/d 1.99	Wet	2
1.00 s/d 1.49	Moderately wet	3
0.99 s/d $-0.99$	Normal	4
$-1.00$ s/d $-1.49$	Moderately dry	5
$-1.50$ s/d $-1.99$	Dry	6
$\leq -2$	Extremely dry	7

**Table 2** | Drought classification based on the frequency of occurrence ([WMO 2012](#))

Drought category	SPEI value	Number of times in 100 years	Severity of event
Moderate dryness	$-1$ s/d $-1.49$	10	1 in 10 years
Severe dryness	$-1.5$ s/d $-1.99$	5	1 in 20 years
Extreme dryness	$\leq -2$	2.5	1 in 50 years

## RESULTS AND DISCUSSION

### The goodness of fit statistics

To prove that the distribution recommended by [Stagge et al. \(2015\)](#) is valid and fits with the spatial conditions of Java Island, it is necessary to evaluate the suitability of the distribution known as the goodness of fit (GOF) statistics. The GOF is conducted to test the fit between the observed results (empirical distribution) and the expected results (theoretical distribution). The main purpose of the GOF is to find out whether the resulting data most likely come from a null distribution. The null distribution is when the tested null hypothesis is true on the statistical test probability distribution. The null hypothesis used in this case states that the theoretical distribution (namely data from the model: gamma distribution for SPI and GEV distribution for SPEI) and the empirical distribution (observational data) come from the same population, then the significance rate used is 95%. The GOF to be evaluated uses three different parameters, namely the KS test, the AD test, and the Cramér-von Mises (CVM) statistical test.

The KS, AD, and the CVM tests are non-parametric suitability tests for two independent samples that are often used to determine whether the null hypothesis is rejected or accepted. The KS test is widely used in statistical testing for two distribution equations because the procedure is relatively simple. This test measures the distance between the two distributions, defined as the difference in the maximum value (the cumulative distribution function minus the empirical distribution function) that may occur (Wijekularathna *et al.* 2019). The greater Kolmogorov distance will decrease the  $p$ -value, and the null hypothesis ( $H_0$ ) is rejected. Hence, the higher  $p$ -value indicates that the covariate distributions of the two matched samples are not statistically different from each other.

Meanwhile, the AD test is a non-parametric statistical procedure that arises from a general distribution function and is not determined by the empirical distribution function (Wijekularathna *et al.* 2019). The hypothesis of this test is that the population of two or more data classes drawn is identical. Each class must be an independent random sample from a population. Basically, the statistical test is carried out by a double sum of integrated squared differences between the empirical distribution functions of the collected sample and the individual samples (Wijekularathna *et al.* 2019).

Then, the CVM test can be measured by the square of the difference between the empirical distribution and the hypothetical cumulative density function (Wijekularathna *et al.* 2019). CVM statistics use half-point correction, taking into account all ordered data points. The distribution of  $F$  under  $H_0$  is uniform at  $(0,1)$ , thus simplifying the calculation. This test takes the dataset as its argument and returns the  $p$ -value so that  $H_0$  will be rejected if the  $p$ -value is  $<0.05$ .

This study investigates time-series datasets (SPI and SPEI) from grid points over Java with different timescales (1–12 months) whether the observation datasets are able to be modelled reasonably by gamma and GEV distributions, respectively. In addition, the datasets are also classified into 12 different months (January–December) separately. Tables 3 and 4 present the number of the grid points (in %) statistically accepted for different timescales and months. In the grid points, the data generated from the theoretical distribution match the empirical distribution data.

In Table 3, the percentage of acceptance rates for the gamma distribution using the KS, AD, and CVM tests

shows values that are not much different from one another. During 12 months (January–December) with varying scales of time, the percentage value tended to fluctuate but was not significant. In general, the number of the grid points statistically accepted is above 93% of Java for all 12 months and different timescales. This indicated that the gamma distribution is suitable to model rainfall amount in Java for different seasons and a variety of timescales.

Similar to the gamma distribution, the GEV distribution is also fit to the observation datasets (rainfall minus evapotranspiration), which is used for the SPEI model. The percentage of acceptance rate among all grid points in Java shows a very high rate. In fact, Table 4 shows that the percentage of acceptance rate tends to be better and more stable than the gamma distribution for the SPI model. This result is supported by Stagge *et al.* (2015), which explains that the level of acceptance of SPEI distribution is higher than SPI, which is caused by the characteristics of the climate water balance that SPEI has, and is not limited by zero precipitation. The parametric distribution is therefore easier to adjust to the distribution of the accumulated climate water balance, which results in the distribution for SPEI having a higher acceptance rate.

### Monthly temporal variation of SPI and SPEI values

Two grid points are selected as the samples of different geographic locations to explain the monthly temporal variation of SPI and SPEI values during the period of 1980–2018. The first grid point is located in Indramayu with the Point ID-30. This location is characterized as a coastal low land area with an elevation of 1 m from mean sea water level (MSWL). This region has an average monthly temperature ranging between 26 and 28.5 °C, a minimum temperature fluctuating from 23.8 to 25.1 °C, a maximum temperature varying from 28.9 to 32.9 °C, and a mean monthly rainfall ranging from 13 to 283 mm. The second grid point is situated in Garut with the Point ID-155. In contrast to the Point ID-30, this place is categorized as a mountainous region with an elevation of 993 m from MSWL. Like other typical mountainous climate regions, this place has lower temperatures but higher amounts of rainfall. This region has an average temperature ranging between 20.2 and 21.3 °C, a minimum temperature of 16.6–18.9 °C, a maximum temperature of

**Table 3** | Percentage of spatial grids in Java for which the Gamma Distribution is accepted to model rainfall amounts (significance level 95%) for 12 months (January–December), different timescales (1–12 months) using three different statistical tests, namely KS, AD, and CVM

		Jan	Feb	Mar	Apr	May	Jun	Jul	Aug	Sep	Oct	Nov	Dec
t1	KS	96.62	99.25	96.99	96.24	95.86	98.87	98.12	98.50	99.25	96.62	94.74	98.50
	AD	96.24	98.50	96.99	95.86	96.24	98.50	98.12	98.87	98.50	98.87	95.86	98.87
	CVM	96.62	98.50	95.86	93.23	96.24	98.87	96.99	97.37	98.87	96.62	94.36	98.50
t2	KS	97.74	97.74	97.37	98.85	96.99	98.87	99.25	98.87	98.50	95.86	94.36	96.24
	AD	98.50	98.87	97.74	98.09	97.37	99.25	99.25	99.25	98.87	96.24	94.74	95.49
	CVM	97.74	98.12	98.12	97.71	96.62	98.87	98.50	98.12	98.87	95.11	93.98	95.11
t3	KS	98.50	96.99	97.74	98.87	98.12	98.87	98.50	98.87	97.74	98.50	97.37	98.12
	AD	98.87	98.50	98.50	98.50	98.50	97.74	99.25	99.25	99.62	98.87	98.12	98.87
	CVM	97.74	97.37	98.12	98.12	98.12	97.37	99.25	99.25	98.87	98.50	97.74	96.99
t4	KS	97.74	98.50	97.74	98.50	97.74	98.50	98.87	98.50	99.25	97.37	96.24	97.74
	AD	97.74	98.50	98.87	98.50	98.87	98.12	98.12	98.87	99.25	97.37	96.99	98.12
	CVM	96.62	98.50	98.50	97.37	98.12	98.50	97.74	98.50	99.25	96.99	96.99	96.62
t5	KS	96.99	97.37	98.50	98.50	99.25	98.50	97.37	99.62	99.62	99.25	96.24	97.74
	AD	98.12	98.50	99.25	98.87	98.87	98.87	98.87	99.25	99.62	98.87	98.12	98.12
	CVM	96.99	97.37	98.87	98.50	98.50	98.87	97.37	99.25	99.62	99.25	98.50	98.12
t6	KS	98.85	98.87	98.50	98.12	97.74	98.87	98.50	98.87	99.25	98.87	97.37	97.74
	AD	99.24	98.50	98.50	98.50	98.87	99.25	99.25	99.62	99.62	98.50	97.37	98.87
	CVM	99.24	98.12	98.12	97.74	98.50	99.25	98.50	99.62	99.25	98.50	97.74	97.74
t7	KS	98.87	98.87	99.62	98.50	98.50	98.50	97.74	97.74	98.12	98.50	99.62	98.50
	AD	98.87	99.25	99.62	98.50	98.50	98.50	98.50	98.12	98.87	99.62	99.62	99.25
	CVM	98.50	98.87	98.87	98.12	98.50	98.87	97.37	98.50	98.50	98.87	98.87	97.74
t8	KS	99.25	98.87	99.25	98.87	97.37	98.50	98.87	98.50	98.50	98.50	98.50	96.99
	AD	99.25	99.25	98.12	99.25	98.12	99.25	98.87	98.50	99.25	99.25	96.99	98.12
	CVM	98.50	99.25	98.12	99.25	97.74	98.87	98.50	98.12	98.50	98.50	97.37	97.74
t9	KS	97.74	97.37	99.62	98.50	98.87	98.12	99.25	98.47	98.50	98.12	99.25	97.74
	AD	98.50	98.12	99.62	98.87	99.25	98.50	99.62	99.62	98.12	98.87	98.50	98.50
	CVM	98.12	97.74	98.87	98.87	99.25	98.50	99.25	99.62	98.50	98.12	98.12	98.12
t10	KS	98.50	98.50	98.50	99.25	98.87	98.12	98.87	97.37	98.12	99.25	98.50	97.71
	AD	99.62	99.25	98.50	98.87	99.25	98.50	99.25	98.50	98.87	99.25	98.50	98.85
	CVM	98.50	98.50	98.50	98.87	99.25	98.12	98.87	98.12	98.50	98.12	98.50	98.85
t11	KS	98.87	98.87	98.87	97.74	99.25	98.50	97.37	98.50	97.74	98.87	96.99	99.62
	AD	99.62	98.50	98.87	98.50	99.25	98.87	98.50	98.12	99.25	98.50	98.50	99.62
	CVM	98.50	98.50	97.74	98.87	98.50	98.12	97.74	98.12	99.25	97.74	99.25	98.87
t12	KS	98.12	98.50	98.87	98.50	99.25	98.87	98.87	98.50	98.87	99.25	98.87	98.12
	AD	98.87	99.25	99.25	98.87	99.25	98.50	99.25	99.62	99.62	98.87	98.87	99.25
	CVM	98.87	98.50	97.74	98.87	99.25	98.12	98.87	98.50	98.12	99.25	99.25	98.87

24.7–25.7 °C, and a mean monthly rainfall ranging from 73 to 517 mm.

In general, drought indices derived by the SPI method present systematically lower than the SPEI approach, particularly for the upper thresholds from  $-1$  to  $-2$  as shown in Figure 4. This means drought severity generated by SPI reveals systematically higher other than SPEI for a given month. Figure 4 presents a monthly temporal variation of drought indices for

both SPI and SPEI during the period of 1980–2018. The blue lines show the SPI values, while the red lines represent the SPEI values. From the figure, it can be seen that the drought indices based on the SPI analyses dominate the lowest margin. The lowest SPI value was around  $-2.964$ , while SPEI was only  $-2.529$  for the Point ID-30. Similarly, for the Point ID-155, the lowest SPI value was  $-3$ , while SPEI was  $-2.69$ . Even at the 175th month, both locations

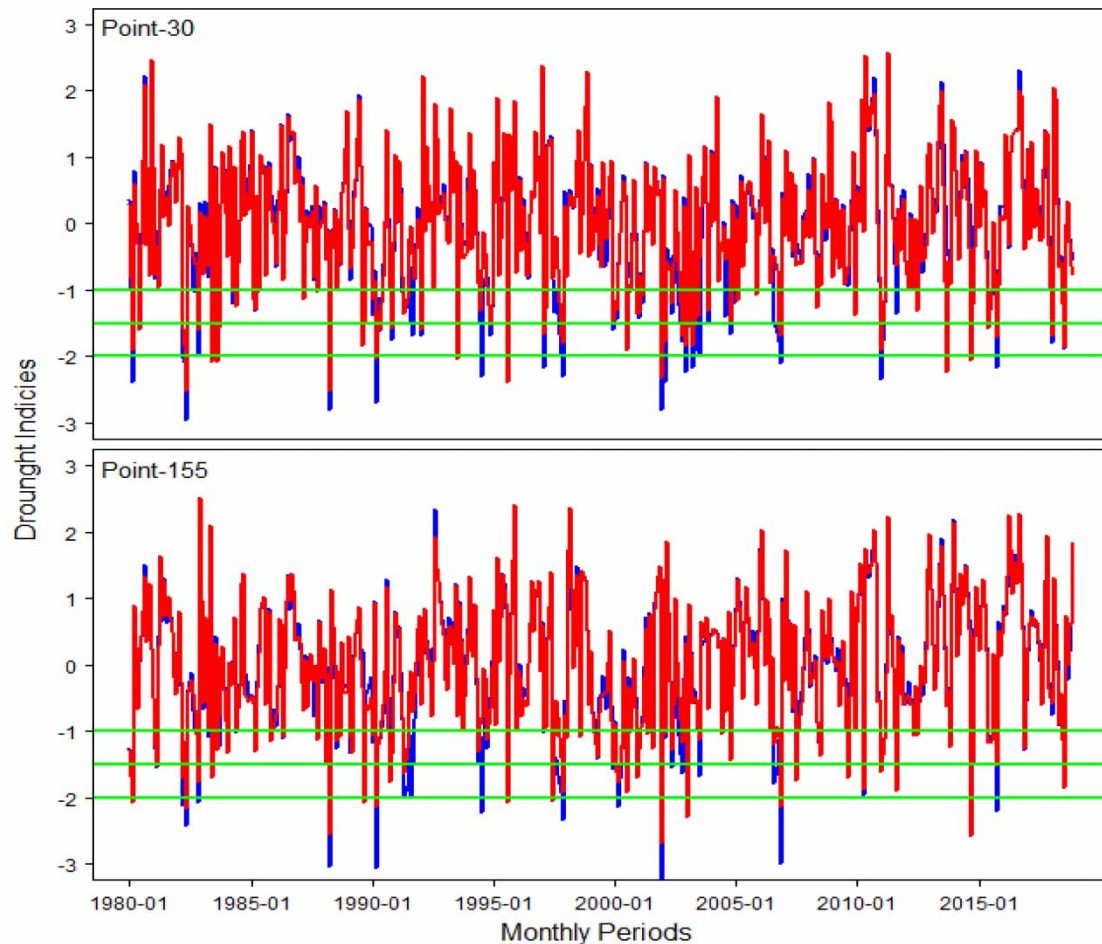
**Table 4** | Percentage of spatial grids in Java for which the GEV distribution is accepted to model rainfall minus evapotranspiration amounts (significance level 95%) for 12 months (January–December), different timescales (1–12 months) using three different statistical tests, namely KS, AD, and CVM

		Jan	Feb	Mar	Apr	May	Jun	Jul	Aug	Sep	Oct	Nov	Dec
t1	KS	99.07	99.53	97.55	99.51	99.07	99.53	99.07	98.53	97.58	97.66	99.05	97.66
	AD	99.07	99.53	99.02	99.51	98.60	99.07	99.53	99.51	99.03	99.53	99.53	98.60
	CVM	98.60	99.53	98.04	99.51	98.60	99.07	97.20	98.53	98.07	98.60	99.53	97.66
t2	KS	98.60	99.02	99.52	99.50	98.56	99.07	99.07	98.59	98.01	99.07	98.58	99.06
	AD	99.07	99.51	99.05	99.50	98.09	99.07	99.07	98.12	98.51	99.07	99.06	98.58
	CVM	99.07	99.02	99.05	98.51	98.56	99.53	97.66	97.18	98.01	98.60	98.58	98.58
t3	KS	99.51	98.58	98.57	99.52	99.01	98.60	99.07	99.07	99.53	98.60	97.66	99.02
	AD	99.51	99.06	98.57	99.52	99.50	99.07	98.13	99.53	99.53	99.53	99.07	99.51
	CVM	99.51	99.06	98.10	99.52	99.50	99.07	98.13	99.07	99.53	99.53	99.07	99.02
t4	KS	99.47	98.58	99.03	99.01	95.52	99.04	99.07	99.07	99.53	98.60	99.07	98.60
	AD	98.95	99.53	99.51	99.51	98.01	99.04	99.53	99.07	99.53	99.53	99.07	99.53
	CVM	98.95	99.05	99.03	99.01	97.01	99.04	99.07	98.60	99.53	98.60	98.13	99.53
t5	KS	99.03	99.48	97.96	99.01	94.95	97.66	98.13	97.66	98.60	99.07	98.13	98.60
	AD	99.52	99.48	99.49	99.01	96.97	99.07	98.60	99.53	99.07	99.53	99.07	99.07
	CVM	99.52	98.43	99.49	99.01	96.97	99.07	98.13	98.13	99.53	99.53	99.07	98.60
t6	KS	97.62	99.52	98.77	99.44	99.03	98.57	98.13	99.53	98.60	98.60	99.53	99.53
	AD	98.57	99.52	98.77	98.89	99.51	98.57	98.60	99.53	99.53	99.07	99.53	99.53
	CVM	98.10	98.56	98.16	98.89	99.03	98.57	99.07	99.53	99.07	98.60	98.13	99.53
t7	KS	98.56	99.53	97.08	99.38	99.48	98.56	97.20	97.66	99.07	98.60	99.53	99.06
	AD	98.56	99.53	97.66	99.38	99.48	99.04	96.73	99.53	99.53	99.53	99.07	99.06
	CVM	98.08	99.53	98.25	99.38	99.48	98.56	96.26	98.13	99.07	99.53	99.07	99.06
t8	KS	99.07	99.52	97.84	95.93	99.48	97.46	99.03	98.59	96.73	98.13	99.07	98.13
	AD	99.53	99.05	99.46	98.84	99.48	99.49	99.52	99.06	97.66	99.07	99.53	99.07
	CVM	99.07	99.05	98.38	98.84	99.48	99.49	99.52	98.59	98.13	99.07	99.53	99.07
t9	KS	98.60	98.60	97.40	98.36	98.96	98.47	98.00	99.02	97.65	99.53	99.53	98.13
	AD	99.53	98.60	97.92	98.36	99.48	99.49	98.50	99.51	99.53	99.53	99.53	99.07
	CVM	99.53	99.07	97.92	97.81	99.48	98.98	98.50	98.04	99.06	99.53	99.53	98.60
t10	KS	99.07	99.07	98.55	98.40	97.50	97.97	99.02	98.97	99.51	97.64	99.07	99.07
	AD	99.53	98.60	98.07	98.93	98.00	98.48	99.02	98.97	99.01	98.11	99.53	99.53
	CVM	99.07	98.60	98.07	99.47	98.00	97.97	98.53	98.46	99.51	97.17	99.07	98.60
t11	KS	97.66	99.07	98.58	99.02	98.97	98.47	99.50	98.50	96.94	99.00	98.04	99.53
	AD	99.07	99.53	99.53	99.51	98.97	98.98	99.01	99.00	98.98	98.01	99.02	99.53
	CVM	98.60	99.53	99.05	99.51	98.97	98.98	99.50	98.50	98.98	98.01	99.02	99.06
t12	KS	98.60	99.51	98.60	98.60	99.52	98.47	99.49	98.49	97.99	98.97	98.99	98.52
	AD	99.07	99.51	99.07	98.60	99.52	98.98	99.49	98.99	98.99	98.97	98.49	99.51
	CVM	99.07	99.51	99.07	98.60	99.52	98.47	98.99	98.99	98.49	98.97	98.99	98.52

showed a significant difference between the SPI and SPEI values. The SPI value at Point ID-30 was  $-2.289$ , while the SPEI value was  $-0.7$  and the SPI and SPEI values at Point ID-155 were  $-2.217$  and  $-0.79$ , respectively.

Apart from showing a lower value, SPI also detected the number of dry months (months of drought) more than SPEI. SPI detected 78 out of 468 months of drought, while SPEI detected 73 months on Point ID-30 (Indramayu). Whereas

from the detection results, the drought incidence based on SPI/SPEI has a match with the actual events from 2003 to 2018 that were recorded by DIBI in June 2003, July 2003, August 2004, November 2006, August 2011, and July 2018. Interestingly, SPI and SPEI detected almost the same number of drought at Point ID-155 (Garut) of 83 and 82 months, respectively. Different from Indramayu, Garut succeeded in detecting more drought events similar to that of



**Figure 4** | The comparison of SPI-1 and SPEI-1 at Point ID-30 (Indramayu) and Point ID-155 (Garut). The vertical axes represent drought indices for SPI (blue lines) and SPEI (red lines). The horizontal axes define months (January 1980–December 2018). Please refer to the online version of this paper to see this figure in colour: [doi:10.2166/wcc.2021.022](https://doi.org/10.2166/wcc.2021.022).

the actual drought in July 2003, October 2004, August 2006, November 2006, June 2008, July 2008, August 2011, and July 2018. This indicates that the SPI approach yields a conservative estimation compared with the SPEI model for both locations. However, in the mountainous region (Garut), SPI and SPEI present quite similar behaviour due to low temperature and high total rainfall.

Nevertheless, temporal variations of both indices exhibit similar patterns. This means that there is a strong correlation between two drought indices. Based on Figure 4, it can be seen that there are several patterns that show one of the lines is far from each other. This pattern difference mostly occurs from April to September (dry season). So, when the dry season comes, the temperature would increase and cause the evaporation to increase, while the rainfall

decreases. With the increase of evaporation rate, the availability of water would decrease which eventually causes an area to become drier. This, in turn, causes SPEI to have a lower value than SPI during the dry season and indicates that temperature may influence the correlation between SPI and SPEI.

These results are supported by a study conducted by Zhang *et al.* (2019). From their research, it was concluded that the frequency of drought would increase, while the correlation decreases with the increased value in temperature. In their research, the frequency of drought decreased from the highest to the lowest margin in summer, autumn, spring, and winter, respectively. However, the results of our research are contradictory to those in Gurrapu *et al.* (2014), as the study concluded that the correlation between

SPI and SPEI was weaker in winter and relatively stronger in summer, autumn, and spring. The correlation between the two analyses during winter was weaker but positive, whereas the correlation in April was weaker and negative, which was probably due to the increased river flow from rapid snowmelt.

The difference in results may be due to different conditions in the study area. In Java, there are only two seasons and there is no snow, so during the dry season, when the temperature increases, the area will become drier. It is different from the study reported in the research by Gurrapu *et al.* (2014), where there is snow in the research location so that with the increasing temperature, the water availability in the area increases due to snowmelt.

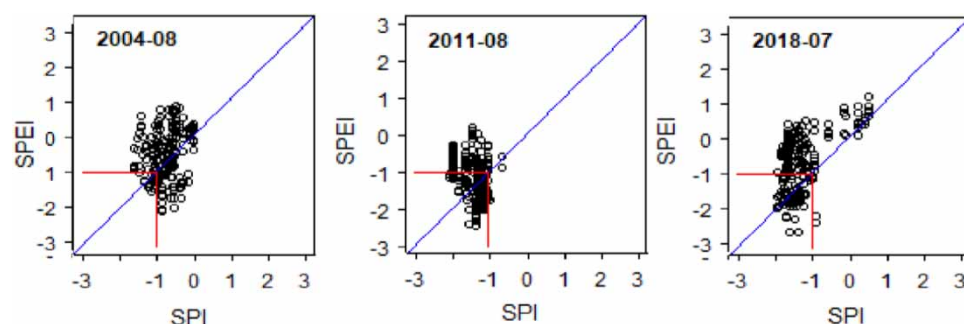
### Comparison of SPI and SPEI values with historical droughts

Three historical drought events were selected as samples to evaluate how reliable SPI/SPEI methods estimate drought events. During the 16 years of recording drought incidents contained in DIBI, the number of drought occurrences that occurred at one time varied greatly. The varying number of drought events can be due to the location of Java Island, which is between two oceans (Pacific and Indian) and two continents (Asia and Australia), which causes a natural phenomenon, namely El Nino. The level of strength of El Nino can be determined through the Oceanic Nino Index (ONI), which is the standard used for NOAA. ONI classifies El Nino into four levels based on sea surface temperature, including weak (0.5–0.9), moderate

(1–1.4), strong (1.5–1.9), and very strong ( $\geq 2$ ). DIBI recorded that the highest number of droughts in Java occurred in August 2004, August 2011, and July 2018, where El Nino with a weak category was also hitting Java.

Therefore, the three drought events that occurred in different years would be discussed. This would later be compared with the historical droughts recorded by DIBI. One point to consider is when the drought event in DIBI is recorded at the beginning of the month, the drought data recorded in the previous month will be used, while those recorded at the end of the month will use the drought data for that particular month. The results of drought analysis in August 2008, August 2011, and July 2018 are as shown in Figure 5.

Spatial distributions among 144 cities/regencies of drought occurrences in August 2004 were under-estimated by both SPEI and SPI methods. Based on Figure 5, the drought events occurred when the dots (cities/regencies) were located below the red lines or the SPI and SPEI values were less than or equal to  $-1$ . Historical drought hazards in August 2004 recorded that 42 cities were suffering drought hazards, including four cities in Banten, 15 cities in West Java, 18 cities in Central Java, one city in Yogyakarta, and four cities in East Java provinces. However, the SPI method detected 25 cities that were facing drought disasters covering three cities in Banten province, five cities in West Java province, 12 cities in Central Java province, and five cities in East Java province. Meanwhile, SPEI methods were applied to 22 cities suffering droughts, including three cities in Banten province, six cities in West Java province, 12 cities in Central Java province, and one city in Yogyakarta province.



**Figure 5** | The spatial distributions of drought events based on SPI and SPEI values for all grid points and for selected drought occurrences (August 2004, August 2011, and July 2018). The vertical axes are drought indices generated by SPEI and the horizontal axes are drought index produced by SPI. Please refer to the online version of this paper to see this figure in colour: [doi:10.2166/wcc.2021.022](https://doi.org/10.2166/wcc.2021.022).

In contrast to August 2004, both SPI and SPEI methods overestimate a number of cities/regencies suffering drought hazard. While the factual drought regions recorded by DIBI were distributed across 39 cities/regencies, the SPEI method predicted 46 cities/regencies hit by drought, and the SPI method estimated 82 cities/regencies. This indicates that SPEI performs better other than SPI. A number of 39 factual drought cities/regencies were distributed in four cities in Banten, 17 cities in West Java, 11 cities in Central Java, and seven cities in East Java provinces. In total, 46 drought cities/regencies estimated by SPEI include six cities in Banten, one city in DKI Jakarta, 18 cities in West Java, 16 cities in Central Java, one city in DI Yogyakarta, and four cities in East Java provinces. In total, 82 drought cities calculated by the SPI model are six cities in Banten, one city in DKI Jakarta, 20 cities in West Java, 24 cities in Central Java, four cities in Yogyakarta, and 27 cities in East Java provinces. SPI performs worst in East Java, while SPEI performs worst in Central Java.

Last, in July 2018, DIBI recorded 62 cities experiencing droughts covering six cities in Banten, 17 cities in West Java, 21 cities in Central Java, two cities in Yogyakarta, and 16 cities in East Java. Interestingly, in this particular month, SPI and SPEI detected the same number of droughts and cities. Both indices successfully detected 70 cities covering six cities in Banten, one city in Jakarta, 20 cities in West Java, 22 cities in Central Java, three cities in Yogyakarta, and 18 cities in East Java.

From these results, it can be seen that on average, SPI usually detects more drought events than SPEI. Even in August 2011, the difference between the two indices was very significant in detecting the number of drought events. To better understand how the characteristics of SPI and SPEI in detecting drought, the following table presents a recapitulation of drought events that occurred in cities or districts. The recapitulation contains the total drought incidents based on DIBI, SPI, and SPEI (Table 5).

The SPI provides an overestimate of events when detecting drought that was very much different from the SPEI and actual drought occurrences. Even though, in several cities, SPEI detected a greater drought event than SPI, the difference in numbers given by the SPEI was relatively low and did not differ much from that of the SPI. This is evidenced by the number of drought events from 2003 to 2018 in 16

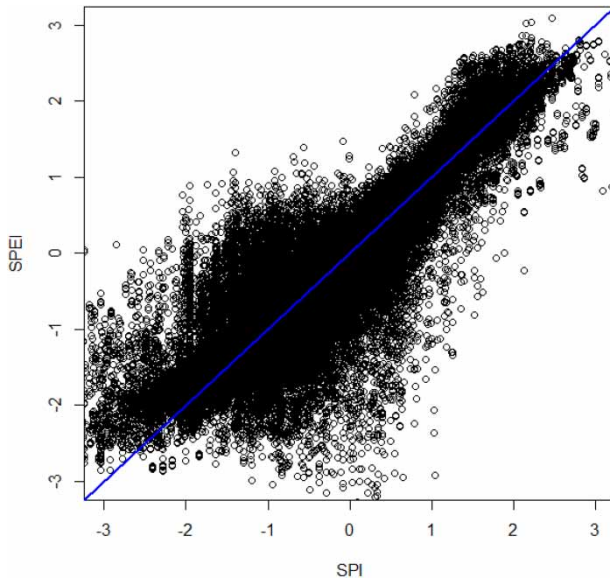
**Table 5** | Recapitulation of drought events from 2003 to 2018 based on DIBI, SPI, and SPEI

City	Total of drought events		
	DIBI	SPI	SPEI
Ponorogo	50	213	80
Bojonegoro	48	200	88
Wonogiri	45	97	102
Nganjuk	40	75	50
Sragen	38	259	120
Kuningan	34	176	52
Semarang	32	63	70
Situbondo	31	176	52
Ciamis	30	38	53
Cirebon	29	75	50
Garut	29	105	86
Tasikmalaya	29	101	48
Bandung	28	45	145
Serang	27	127	94
Indramayu	26	38	28
Sumedang	26	259	120

cities, which are presented in Table 5. When compared with DIBI, the highest estimate given by the SPI for the Sragen district was 221 events, while the lowest estimate was for the Ciamis district with as many as eight drought events. The highest estimate given by SPEI occurred in Bandung city with a total drought of 117 events, then the lowest estimate was two events that occurred in the Indramayu city. This indicates that SPI is very conservative and SPEI is more moderate in estimating drought events.

### Effect of different timescales on similarity of the SPI and SPEI

A scatter plot was used for analysing between SPI and SPEI for determining how closely both indices are related. There was a significant positive correlation between SPI and SPEI, which is seen from the tendency of the data to gather around the diagonal line. The results of the correlation analysis are set out in Figure 6. The SPI and SPEI can actually be used to calculate the drought index for a variety of different timescales. In this study, a different timescale will be used ranging from 1 to 12 months. Most studies have only used

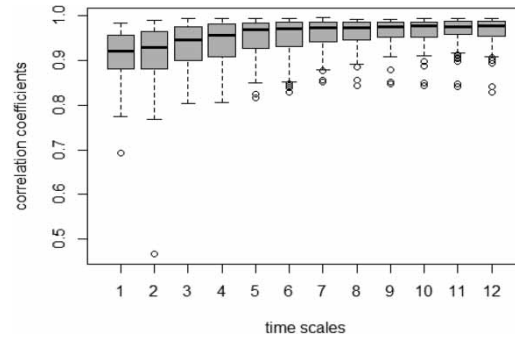


**Figure 6** | Scatter plot of SPI and SPEI values for all grid points and all timescales (1–12 months).

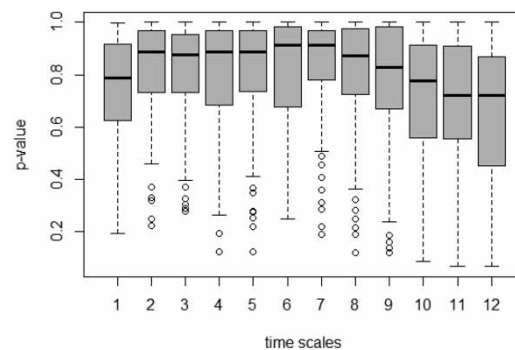
fewer timescales such as 1, 3, 6, and 12 months, while this study has the advantage of being more detailed in order to see the correlation between SPI and SPEI.

To determine more detail about the relationship between SPI and SPEI which was on different timescales, the correlation coefficient and the KS test were used. The difference in SPI and SPEI values may be due to differences in data variables used as input to calculate the drought index. For example, in the event of the same drought, the SPI index may show a value of 1, while the SPEI may show a value of 3. This is possible because the SPI only calculates drought events based on the rainfall rate, while the SPEI identifies drought events not only based on the rainfall rate but also the evapotranspiration of the region. This view is supported by [Gurrapu et al. \(2014\)](#) who write that the differences in the variables used as input data in analysing drought will affect the value of the drought index.

The correlation between SPI and SPEI is consistently increasing along with the longer the timescale used. It can be seen from the box plot in [Figure 7](#) that the value of the correlation coefficient is above 0.9 for all timescales. This showed that the relationship between SPI and SPEI is strong. The 1- to 6-month timescale tends to have a higher significant increase in the correlation coefficient value than the 7- to 12-month timescale, which has a slight



**Figure 7** | Boxplot of the Pearson correlation coefficient between SPI and SPEI values for all grid points during the period of 1980–2018 at different timescales (from monthly to yearly).



**Figure 8** | Boxplot of KS test ( $p$ -value with significance level 5%) between SPI and SPEI values for all grid points during the period of 1980–2018 at different timescales (from monthly to yearly).

increase in the value of the correlation coefficient. Then, in [Figure 8](#) that depicts the results of the KS Test, the  $p$ -value in the 1- to 2-month timescale tends to have a significant increase and then becomes stable up to the 7-month timescale. However, in the 8-month timescale, the  $p$ -value continues to decline up to the 12-month timescale. This indicates that the timescale for the long term is better than the short to medium term.

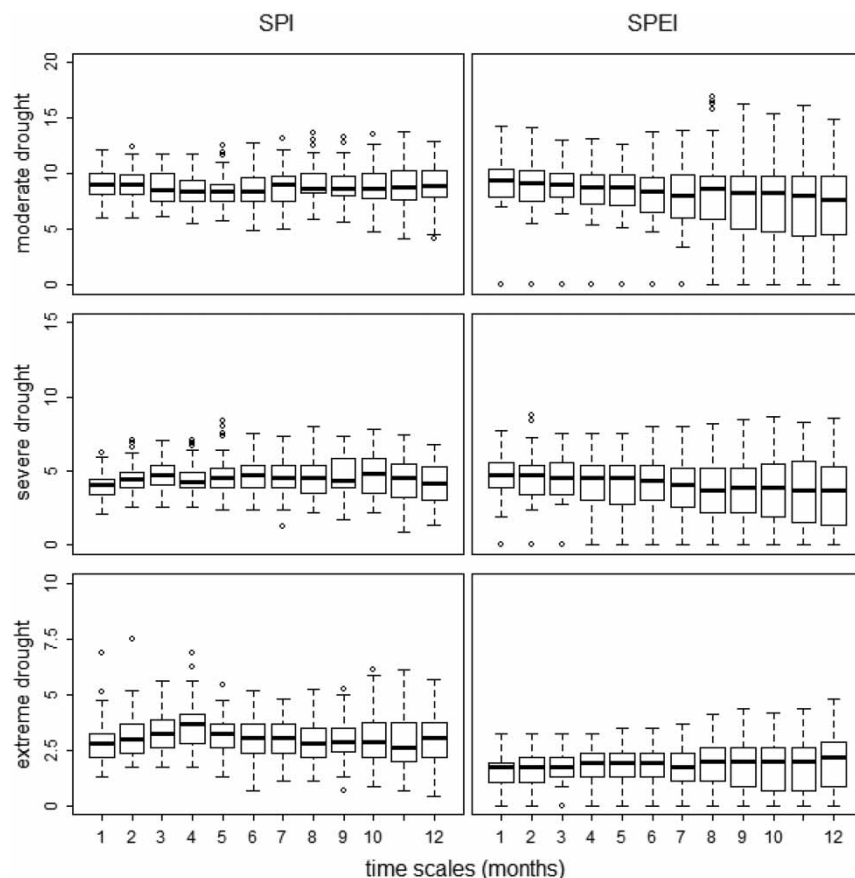
For the drought index, especially from the SPI and SPEI analyses, the use of different timescales will result in different implications from one another ([Nam et al. 2015](#)). Thus, those calculations of drought with different timescales are often used as information to determine water resources management policies in the short, medium, and long term. The timescales that are often used to measure drought

values are 1-, 3-, 6-, and 12-month timescales. The drought index with a 1-month timescale is included in the short-term period, the 3- and 6-month timescale is included in the medium-term period, and the 12-month timescale is included in the long-term period (Nam et al. 2015). The 1-month timescale is more suitable for identifying soil moisture conditions, the 3-month timescale is better for predicting seasonal rain conditions, and the 6- and 12-month timescales are more appropriate for determining the impact of drought on water availability in rivers, ponds, or reservoirs.

### Drought frequency value

In addition to the SPI and SPEI values, this research also discussed the frequency of drought events. Drought events are categorized into three, namely moderate drought

which is included in class 5, severe drought which is included in class 6, and extreme drought which belongs to class 7. The frequency of moderate drought is the percentage of the number of events that have the SPI/SPEI value of  $-1.00$  to  $-1.49$ , which is then divided by the total drought events (which have the SPI/SPEI value of  $-1.00$  to  $-3.00$ ). The frequency of severe drought is the percentage of the number of events that have the SPI/SPEI value of  $-1.50$  to  $-1.99$ , which is later divided by the total number of drought events. The frequency of extreme drought is the percentage of the number of events that have the SPI/SPEI value of  $-2.00$  to  $-3.00$ , which is then divided by the total drought events. As for the frequency value for moderate, severe, and extreme droughts, it is based on the SPI with a timescale of 1–12 months. The percentage of moderate, severe, and extreme drought frequencies based on the SPI and SPEI for all timescales can be seen in Figure 9.



**Figure 9** | Boxplot of frequencies (the number of events) of moderate, severe, and extreme droughts (%) for both SPI and SPEI for all grid points during the period of 1980–2018 at different timescales (from monthly to 12 months).

The frequency rate for SPI will fluctuate more, as the severity of drought increases with the timescale used, whereas for the SPEI with the timescale used, the more severe the level of drought, the more stable the frequency rate. The results of moderate, severe, and extreme droughts are presented in Figure 9. It can be seen that for moderate drought, the highest frequency based on the SPI was 12.18%, while based on the SPEI was 14.32%. Then, the highest frequency, for severe drought, based on the SPI was 6.2%, while based on the SPEI was 7.69%. Meanwhile, for extreme drought, the highest frequency based on the SPI was 6.84%, while based on the SPEI was 3.21%. SPEI has a higher frequency for moderate and severe droughts than SPI, while for extreme drought, the frequency generated by SPI is higher. This indicates that in detecting drought, SPI assesses drought at a more severe level than SPEI.

From the above explanation, it can be concluded that in general the frequency rate for the SPEI is much more stable than that for the SPI, and the drought frequency produced by the SPEI is higher than that by the SPI. With regard to two of the three types of drought frequency, moderate and severe, the SPEI recorded a drought frequency value higher than the SPI. This is due to the existence of the evapotranspiration variable in the SPEI. This feature allows identifying drought events even when the rainfall is not available, so that the index can still be used to capture drought events and calculate the frequency of drought events. Meanwhile, the SPI's extreme drought frequency is higher than that of the SPEI's. Furthermore, the pattern shown for the change in the frequency value against time caused by the SPI and SPEI marks one thing in common, namely the possibility of fluctuations for all types of drought. However, overall the SPEI's drought frequency is more stable than that of the SPI's.

These results are supported by research conducted by Tirivarombo *et al.* (2018). The study found that the SPI was superior in capturing extreme drought events compared with the SPEI. The reason is that when identifying drought that only considers the variable of rainfall, the SPI of which input data are only the rainfall variable will be better to identify extreme drought than the SPEI. The results of the correlation analysis between the SPI and SPEI clearly show that rainfall is the main cause of the drought. It should be noted that the existence of PET becomes important at longer timescales since the correlation is stronger.

## CONCLUSIONS

The conclusions drawn from the results and discussions can be explained as follows.

A comparison between the SPI and SPEI values to temporal variation shows that the correlation between the two indices is quite high for all months for the 1-month timescale. However, this correlation has decreased in the dry months (dry season). In almost all months, the SPI and SPEI values have similar margins with no significant difference, and the SPI value is always below the SPEI value. Yet, in the dry months, the SPEI value is far below the SPI value. This indicates that the temperature variable affects the correlation between the SPI and SPEI because during the dry season the evaporation rate increases more rapidly, resulting in a lower SPEI value than in normal conditions.

The SPI is more conservative in detecting drought than the SPEI. This is indicated by the fact that the SPI detects an overestimation compared with the SPEI and historical data on drought events in Indonesia. Besides, the difference in the timescale used in the analysis will affect the correlation between the SPI and SPEI. The correlation between the SPI and SPEI will get stronger as the timescale used increases.

Then for moderate and severe droughts based on the SPEI, the SPEI shows a higher frequency than the SPI, while for extreme drought, the frequency shown by the SPI is higher. This is because when drought takes into account only the rainfall, the SPI that has one indicator in the form of rainfall will be better at identifying extreme drought than SPEI. The results of the correlational analysis between the SPI and SPEI clearly show that rainfall is the main cause of drought. However, evaporation indicators are also important, especially on a longer timescale where their existence affects the correlation between the SPI and SPEI.

By comparing the two indices, it can be seen how the characteristics and correlations between the SPI and SPEI are. Also, we could identify further the influence of precipitation and evaporation parameters in analysing drought in Java Island. Therefore, this research is expected to be one of the sources of information that can help related parties, especially the BMKG in monitoring drought in Indonesia.

## DATA AVAILABILITY STATEMENT

All relevant data are included in the paper or its Supplementary Information.

## REFERENCES

- Blauhut, V. 2020 [The triple complexity of drought risk analysis and its visualisation via mapping: a review across scales and sectors](#). *Earth-Science Reviews* **210**, 103345. <https://doi.org/10.1016/j.earscirev.2020.103345>.
- BPS 2019 *Indonesia's Product, Harvested Area, and Rice Productivity in 2019*. Indonesian Statistics, Jakarta.
- Gebremeskel, G., Tang, Q., Sun, S., Huang, Z., Zhang, X. & Liu, X. 2019 [Droughts in East Africa: causes, impacts, and resilience](#). *Earth-Science Reviews* **193**, 146–161. <https://doi.org/10.1016/j.earscirev.2019.04.015>.
- Ghorbani, M. A., Kazempour, R., Chau, K. W., Shamshirband, S. & Ghazvinei, P. T. 2018 [Forecasting pan evaporation with an integrated artificial neural network quantum-behaved particle swarm optimization model: a case study in Talesh, Northern Iran](#). *Engineering Applications of Computational Fluid Mechanics* **12** (1), 724–737. <https://doi.org/10.1080/19942060.2018.1517052>.
- Gurrapu, S., Chipanshi, A., Sauchyn, D. & Howard, A. 2014 Comparison of the SPI and SPEI on predicting drought conditions and streamflow in the Canadian prairies. In: *28th Conference on Hydrology and the 26th Conference on Climate Variability and Change, 2010*, p. 7.
- Holden, Z. A., Jolly, W. M., Swanson, A., Warren, D. A., Jencso, K., Maneta, M. & Landguth, E. L. 2019 [A topographically resolved wildfire danger and drought monitoring system for the conterminous United States](#). *Bulletin of the American Meteorological Society* **100** (9), 1607–1613. <https://doi.org/10.1175/BAMS-D-18-0178.1>.
- Jati, M. I. H., Suroso & Santoso, P. B. 2019 Prediction of flood areas using the logistic regression method (case study of the provinces Banten, DKI Jakarta, and West Java). *Journal of Physics: Conference Series* **1367** (1), 012087.
- Martens, B., Miralles, D. G., Lievens, H., Fernández-Prieto, D. & Verhoest, N. E. C. 2016 [Improving terrestrial evaporation estimates over continental Australia through assimilation of SMOS soil moisture](#). *International Journal of Applied Earth Observation and Geoinformation* **48**, 146–162. doi:10.1016/j.jag.2015.09.012.
- Martens, B., Miralles, D. G., Lievens, H., Van Der Schalie, R., De Jeu, R. A. M., Fernández-Prieto, D. & Verhoest, N. E. C. 2017 [GLEAM v3: satellite-based land evaporation and root-zone soil moisture](#). *Geoscientific Model Development* **10** (5), 1903–1925. <https://doi.org/10.5194/gmd-10-1903-2017>.
- McKee, T. B., Doesken, N. J. & Kleist, J. 1993 The relationship of drought frequency and duration to time scales. In *Proceedings of the 8th Conference on Applied Climatology* **17** (22), 179–183.
- Monish, N. T. & Rehana, S. 2020 [Suitability of distributions for standard precipitation and evapotranspiration index over meteorologically homogeneous zones of India](#). *Journal of Earth System Science* **129** (1). <https://doi.org/10.1007/s12040-019-1271-x>.
- Nam, W. H., Hayes, M. J., Svoboda, M. D., Tadesse, T. & Wilhite, D. A. 2015 [Drought hazard assessment in the context of climate change for South Korea](#). *Agricultural Water Management* **160**, 106–117. <https://doi.org/10.1016/j.agwat.2015.06.029>.
- Pang, J., Zhang, H., Xu, Q., Wang, Y., Wang, Y., Zhang, O. & Hao, J. 2020 [Hydrological evaluation of open-access precipitation data using SWAT at multiple temporal and spatial scales](#). *Hydrology and Earth System Sciences* **24** (7), 3603–3626. <https://doi.org/10.5194/hess-24-3603-2020>.
- Peng, J., Dadson, S., Hirpa, F., Dyer, E., Lees, T., Miralles, D. G. & Funk, C. 2020 [A pan-African high-resolution drought index dataset](#). *Earth System Science Data* **12** (1), 753–769. <https://doi.org/10.5194/essd-12-753-2020>.
- Shahid, M. & Rahman, K. U. 2020 [Identifying the annual and seasonal trends of hydrological and climatic variables in the Indus Basin Pakistan](#). *Asia-Pacific Journal of Atmospheric Sciences*. <https://doi.org/10.1007/s13143-020-00194-2>.
- Shamshirband, S., Hashemi, S., Salimi, H., Samadianfard, S., Asadi, E., Shadkani, S. & Chau, K. W. 2020 [Predicting Standardized Streamflow index for hydrological drought using machine learning models](#). *Engineering Applications of Computational Fluid Mechanics* **14** (1), 339–350. <https://doi.org/10.1080/19942060.2020.1715844>.
- Shawul, A. A. & Chakma, S. 2020 [Suitability of global precipitation estimates for hydrologic prediction in the main watersheds of Upper Awash basin](#). *Environmental Earth Sciences* **79** (2), 1–18. <https://doi.org/10.1007/s12665-019-8801-3>.
- Stagge, J. H., Tallaksen, L. M., Gudmundsson, L., Van Loon, A. F. & Stahl, K. 2015 [Candidate distributions for climatological drought indices \(SPI and SPEI\)](#). *International Journal of Climatology* **35** (13), 4027–4040. <https://doi.org/10.1002/joc.4267>.
- Stampfli, A., Bloor, J. M. G., Fischer, M. & Zeiter, M. 2018 [High land-use intensity exacerbates shifts in grassland vegetation composition after severe experimental drought](#). *Global Change Biology* **24** (5), 2021–2034. <https://doi.org/10.1111/gcb.14046>.
- Sun, Q., Miao, C., Duan, Q., Ashouri, H., Sorooshian, S. & Hsu, K. L. 2018 [A review of global precipitation data sets: data sources, estimation, and intercomparisons](#). *Reviews of Geophysics* **56** (1), 79–107. <https://doi.org/10.1002/2017RG000574>.
- Tirivarombo, S., Osupile, D. & Eliasson, P. 2018 [Drought monitoring and analysis: Standardised Precipitation Evapotranspiration Index \(SPEI\) and Standardised Precipitation Index \(SPI\)](#). *Physics and Chemistry of the Earth* **106**, 1–10. <https://doi.org/10.1016/j.pce.2018.07.001>.
- Umiati, T., Suroso & Ardiansyah. 2019 Spatial analysis and monitoring of drought using Standardized Precipitation

- Index in East Java. *Journal of Physics: Conference Series* **1367** (1), 012088.
- Wang, H. & Asefa, T. 2019 [Drought monitoring, mitigation, and adaptation](#). In: *Extreme Hydrology and Climate Variability: Monitoring, Modelling, Adaptation and Mitigation*. <https://doi.org/10.1016/B978-0-12-815998-9.00036-1>.
- Wang, L., Yu, H., Yang, M., Yang, R., Gao, R. & Wang, Y. 2019 [A drought index: the standardized precipitation evapotranspiration runoff index](#). *Journal of Hydrology* **571**, 651–668. <https://doi.org/10.1016/j.jhydrol.2019.02.023>.
- Wijekularathna, D. K., Manage, A. B. W. & Scariano, S. M. 2019 [Power analysis of several normality tests: a Monte Carlo simulation study](#). *Communications in Statistics: Simulation and Computation*, 1–17. <https://doi.org/10.1080/03610918.2019.1658780>.
- World Bank 2019 *Indonesia Economic Quarterly, December 2019: Investing in People*. World Bank, Washington, DC.
- World Meteorological Organization 2012 *Standardized Precipitation Index User Guide* (M. Svoboda, M. Hayes & D. Wood, eds.). World Meteorological Organization, Geneva, Switzerland.
- Zhang, Y., Wang, J., Shen, Z. & Xie, X. 2019 [Evolution characteristics of seasonal drought in hunan based on the standardized precipitation index \(SPI\)](#). *Geoscience and Remote Sensing* **2**, 56–64. <https://doi.org/10.23977/geors.2019.21004>.

First received 19 January 2021; accepted in revised form 29 April 2021. Available online 18 May 2021

# Drought detection in Java Island based on Standardized Precipitation and Evapotranspiration Index (SPEI)

*by* Ardiansyah Ardiansyah

---

**Submission date:** 09-Jul-2022 08:24PM (UTC+0700)

**Submission ID:** 1868311711

**File name:** jwc0122734.pdf (857.94K)

**Word count:** 12138

**Character count:** 57530

## Drought detection in Java Island based on Standardized Precipitation and Evapotranspiration Index (SPEI)

Surosq Dede Nadhilah, Ardiansyah and Edvin Aldrian

### ABSTRACT

This study reports a drought analysis which was carried out using the Standardized Precipitation and Evapotranspiration Index (SPEI) to determine the spatial and temporal level of drought risk in Java, Indonesia. Apart from using the SPEI, this study also used the SPI (Standardized Precipitation Index) as a comparison in detecting drought and also validated with historical drought occurrences. Temporal variations of SPI and SPEI values were discussed by considering different timescales (monthly to yearly). Pearson's correlations between both drought indices were calculated to see how similar both indices were. Also, the Kolmogorov–Smirnov tests were used for the similarity test of two kinds of distributions. The results obtained from this analysis showed that the correlation coefficient between the SPI and SPEI models was relatively high on a monthly scale and consistently increased along with the increase of temporal scales but had a decreasing trend during the dry season. However, the SPI detected drought severity with an excessively high estimate in comparison with the SPEI. Greater spatial extents of drought estimation were also generated by SPI followed by SPEI in comparison to factual drought occurrences. As a consequence, SPEI becomes more moderate and SPI as a conservative approach for estimating drought events.

**Key words** | drought, Indonesia, Java Island, SPEI

### HIGHLIGHTS

- The drought severity generated by SPI is revealed to be systematically higher than SPEI for most of the given month period.
- In detecting drought, SPI is very conservative, while SPEI is moderate.
- The correlation between SPI and SPEI will be stronger if the timescale used is longer.
- Rainfall is the main cause of the drought, but the existence of evapotranspiration becomes important for a longer timescale.

**Surosq** (corresponding author)

**Nadhilah**  
Department of Civil Engineering, Faculty of  
Engineering,  
Jenderal Soedirman University,  
Purwokerto,  
Indonesia  
E-mail: surosotsipi@unsoed.ac.id

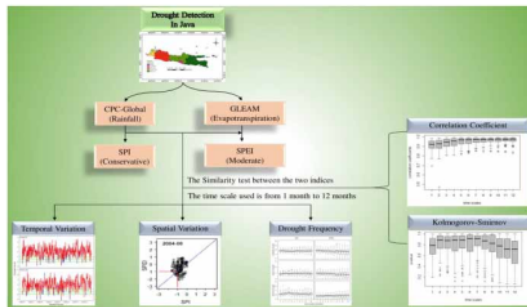
**Ardiansyah**  
Department of Agricultural Engineering, Faculty of  
Agricultural,  
Jenderal Soedirman University,  
Purwokerto,  
Indonesia

**Edvin Aldrian**  
Agency for the Assessment and Application of  
Technology (BPPT),  
Jakarta,  
Indonesia

This is an Open Access article distributed under the terms of the Creative Commons Attribution Licence (CC BY 4.0), which permits copying, adaptation and redistribution, provided the original work is properly cited (<http://creativecommons.org/licenses/by/4.0/>).

doi: 10.2166/wcc.2021.022

## GRAPHICAL ABSTRACT



## INTRODUCTION

Drought is a natural phenomenon that occurs as a result of a high rainfall deficit (Wang & Asefa 2019). This later influences the agricultural sector in Indonesia directly. It was reported by Indonesian Statistics (BPS) that the potential financial loss due to drought in agriculture is estimated at three trillion rupiahs per year (BPS 2019). Additionally, beside having a direct impact on decreasing food productivity, drought can also have indirect environmental impacts, such as forest fires (Holden et al. 2019).

According to data from the Ministry of Environment and Forestry, the total number of forest fires in 2019 reached 1,649,258 hectares, a significant increase from the total of forest fires in 2018 of 529,266 hectares. In September 2019, it was reported by the National Disaster Management Agency (BNPB) that more than 900,000 people experienced respiratory problems due to smoke resulting from forest fires (World Bank 2019). Meanwhile, throughout 2019, Indonesia's total losses due to forest and land fires reached US\$ 5.2 million (Rp. 72.95 trillion), which was equivalent to 0.5% of Indonesia's Gross Domestic Product (GDP) (World Bank 2019). Next, based on water availability data in 2019 compiled by the Research and Development Center for Water Resources of the Ministry of Public Works and Public Housing (PUPR), the availability rate of water for one person in Java Island is 1,169 m<sup>3</sup>/year and will continue to decline until 2040 when the availability rate of water for

one person is limited to 476 m<sup>3</sup>/year, which is categorized as severe scarcity. Having the potential to cause severe impacts, drought has become a disaster that has received serious attention at both national and international levels, since it greatly affects people's activities in various sectors of life (Stampfli et al. 2018).

Drought that occurs slowly (called slow on-set drought) may have a severe long-term impact on various sectors of human life that needs to be anticipated. Therefore, mitigation efforts are needed to reduce any potential impacts of drought (Gebremeskel et al. 2019). One of the non-structural mitigation strategies that can be conducted is implementing early detection systems to monitor drought by creating a disaster risk distribution map. Disaster risk mapping is a starting point for raising public awareness, informing policy-makers or authorities to encourage disaster management (Blauhut 2020).

In an early detection system, understanding the characteristics of drought is imperative. By identifying and representing drought characteristics and indicators, a drought index or a combination of drought indices is usually used (Blauhut 2020). A drought index consists of several drought indicators that can explain quantitatively the intensity, duration, and severity of drought (Wang & Asefa 2019). Drought events can be analysed because several drought indices have been developed to detect and monitor drought

events (Wang *et al.* 2019). Two drought indices that are often used for drought analysis are the Standardized Precipitation Index (SPI) and the Standardized Precipitation and Evapotranspiration Index (SPEI).

SPI is a drought index that has been standardized to measure rainfall anomalies and is the main indicator of drought recommended by the World Meteorological Organization (Stagge *et al.* 2015). The precipitation data used in this research is obtained from Global Precipitation, which has the advantage of providing precipitation data for a long time period from 1979 to 2020. The data are available almost in real-time for a whole continent so that the quality of the data is confirmed to be very good, in terms of both spatial and temporal coverages. The study location focuses on Java Island because according to the data compiled by the meteorological, climatological, and geophysical agency (BMKG), Java Island has been the island with the highest frequency of being hit by drought compared with the other islands in Indonesia for 30 years from 1979 to 2009 and is still prone to experiencing drought until now.

Beside that, the utilization of SPI and SPEI as the drought indices in this study is because these two indices are most often used, especially SPI as the main parameter in monitoring drought in Indonesia by the BMKG. The use of SPI as a comparison index is due to the existence of the same parameter as SPEI in analysing drought, namely precipitation. Additionally, apart from SPI and SPEI, there are various types of drought indices that are developed to suit the conditions of certain areas. One of them is the Hurst index, which is developed to determine annual and seasonal trends with hydrological and climatic variables in streamflow (Shahid & Rahman 2020).

The paper is divided into four sections, namely Introduction, Methods, Results and discussion, and Conclusions. The first section describes the introduction of why this study is essential to conduct, the study location, and data available. Then, the methods of SPEI and SPI approaches as well as drought classification are explained in the section 'Methods'. Some research findings, such as behaviours of SPI and SPEI methods, for detecting droughts in terms of temporal and spatial characteristics are discussed in the section 'Results and discussion'. Finally, in the section 'Conclusions', the conclusion gives a brief summary of the findings and their implications.

## Study location

The study location was Java Island, which is situated between 113°48'10" to 113°48'26" East Longitude and 7°50'10" to 7°56'41" South Latitude as shown in Figure 1. Java Island has a total area of 138,793 km<sup>2</sup> with a length from east to west of 1,033 km, and within its central position, it has a width of about 104 km, while in the western part, the width is about 98 km and the eastern part is about 107 km. Administratively, Java Island consists of six provinces: four provinces include Banten with the provincial capital of Serang, West Java with the provincial capital of Bandung, Central Java with the provincial capital of Semarang, and East Java with the provincial capital of Surabaya; two special areas at the provincial level, namely Jakarta and Yogyakarta. Furthermore, Banten province consists of six districts/cities, Jakarta province consists of five municipalities, West Java province consists of 25 districts/cities, Central Java province consists of 35 districts/cities, Yogyakarta province consists of five districts/cities, and East Java province consists of 38 districts/cities.

Java Island has an annual average temperature of 22°–29 °C, and usually during the day and the dry season, the temperature in the coastal area can reach up to 34 °C, while the average humidity is around 75%. Meanwhile, the annual rainfall ranges from 1,773 to 3,710 mm. Based on the distribution of average monthly rainfall, Java Island has a monsoon type that makes it experience only two seasons, namely the dry season that occurs from April to September (dry months) and the rainy season that occurs from October to March (wet months).

## Drought historical data

To anticipate the occurrence of drought, future projections could be carried out to determine the recurring drought period by utilizing historical data. Drought historical data are recorded data from reports of previous droughts that have occurred in a certain time period. Drought historical data of Java were obtained through the Indonesian Disaster Information Data (DIBI) recorded by the National Disaster Management Agency (BNPB), and the available data taken were from 2003 to 2019. These data contained coordinates

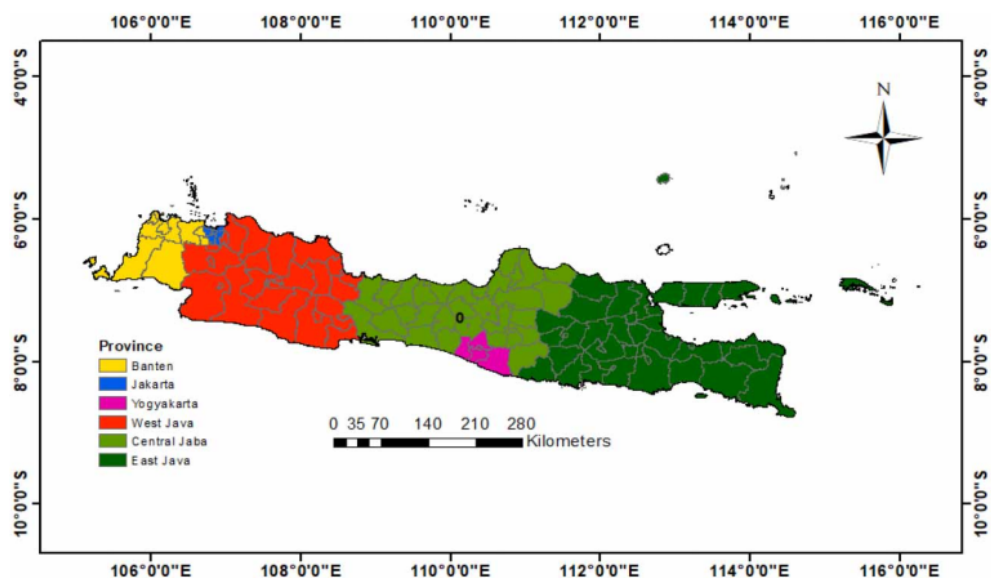


Figure 1 | Map of Java Island.

of the location, name of the district/city and province, number of victims (injured, died, evacuated, and missing), material losses, and a description of the events that were recorded directly at the disaster site. Drought historical data would be used for validation coupled with the results of the SPI and SPEI analyses to identify a correlation between the two. As for the total data on drought events in Java Island, it is illustrated by Figure 2.

#### Precipitation data

In this research, precipitation data were obtained from Global Daily Precipitation (CPC-Global). CPC-Global was developed by the National Oceanic and Atmospheric Administration (NOAA), which is the first product of the CPC Unified Precipitation Project (Sun *et al.* 2018). This project is devoted to creating an integrated set of precipitation

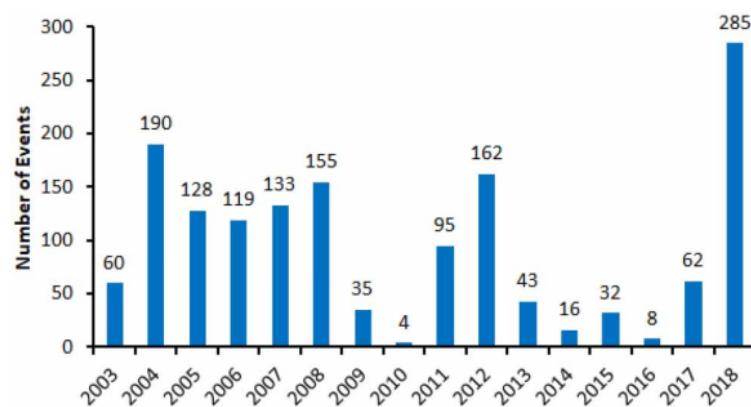


Figure 2 | Total event of drought in Java Island.

products that have consistent quantity and improved quality using the optimal interpolation objective analysis technique by combining all available sources of information in the CPC-Global (Sun *et al.* 2018). CPC-Globa has been constructed over the global land areas, with the gauge reports from over 30,000 stations collected from multiple sources, including GTS (Global Telecommunication System), COOP (Cooperative Observer Network), and other national meteorological agencies (Sun *et al.* 2018).

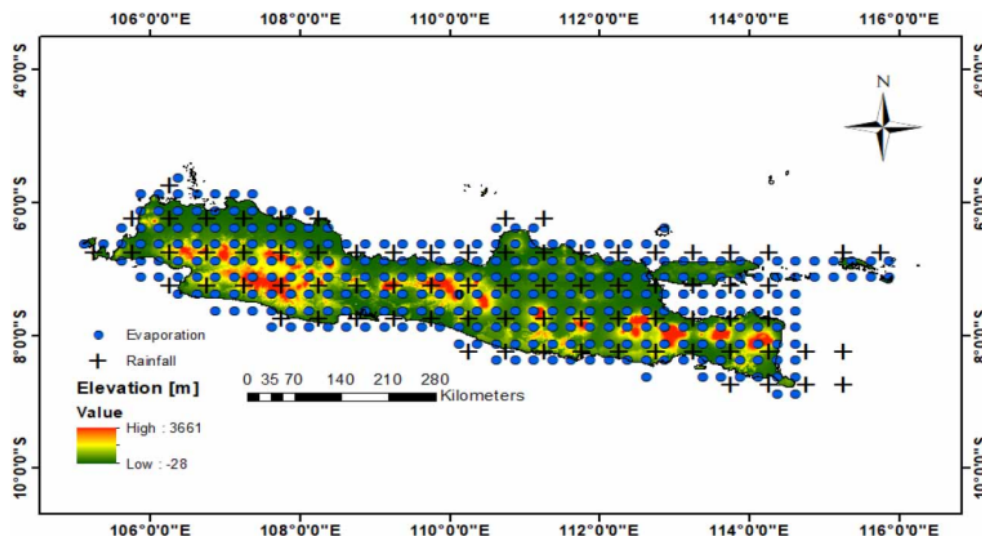
The use of precipitation data from CPC-Globa has been widely used for various types of research, especially for predicting hydrological variability and water balance. CPC-Globa is used to simulate river flow variability on daily and monthly timescales in the watershed (Shawul & Chakma 2020), a simulation to estimate the effective hydrological processes in the watershed (Pang *et al.* 2020). Even CPC-Globa is recommended as precipitation data for use in extreme drought analysis, future climate analysis, and hydrological modelling (Pang *et al.* 2020) and can be useful as a source of precipitation data for hydrological modelling in the tropical regions, where precipitation data are scarce (Shawul & Chakma 2020).

Furthermore, CPC-Globa is able to provide daily precipitation data, while in drought analysis, the timescale used is

monthly. Therefore, the daily precipitation data would be accumulated into monthly data. To analyse drought based on SPEI, the form of data used is usually that which comprises more than 40 years, and the data from CPC-Globa have fulfilled the requirement in this regard. In contrast to data from satellites such as Tropical Rainfall Measuring Mission (TRMM) (Jati *et al.* 2019; Umiati *et al.* 2019) which only provides data for about 20 years, the quality of Global Precipitation data is said to be better and more reliable. Moreover, the data from CPC-Globa have a grid resolution of  $0.5^\circ \times 0.5^\circ$ . Since the grid size for precipitation is different from the evaporation grid size ( $0.25^\circ \times 0.25^\circ$ ), the precipitation grid size was converted into the evaporation grid size first. The following illustration is the image for the precipitation and evaporation data grids (Figure 3).

#### Evaporation data

Apart from precipitation, evaporation is an integral component that is used to detect changes in the hydrological cycle and estimate the impact of climate change on water resources (Ghorbani *et al.* 2018). In this research, the evaporation data were obtained from GLEAM (Global Land-surface Evaporation: the Amsterdam Methodology).



**Figure 3** | The investigation location: Java Island, Indonesia. Black plus signs represent precipitation grid points. Blue dots represent evaporation grid points. Please refer to the online version of this paper to see this figure in colour: [doi:10.2166/wcc.2021.022](https://doi.org/10.2166/wcc.2021.022).

GLEAM data sets have already been comprehensively validated against an extensive set of *in situ* observations. A global validation using a large database of *in situ* measurements of evaporation had been conducted from 91 eddy covariance towers (FLUXNET observations). Moreover, soil moisture measurements from 2,325 *in situ* sensors from the database of the International Soil Moisture Network (ISMN) had been taken for further validation.

The GLEAM data sets have also been evaluated over continental Australia (south of Java Island), where they generally perform better (Martens *et al.* 2016, 2017). Especially, GLEAM data have been applied in several regions/countries such as in Africa (Peng *et al.* 2020) and Australia (Martens *et al.* 2016), which are used for multiple hydro-meteorological applications such as to anticipate the availability of water and food due to drought (Peng *et al.* 2020) and for modelling the land water availability on terrestrial evaporation fields (Martens *et al.* 2016). Hence, the evaporation data sets derived from the GLEAM are reasonably used for further analysis in this study.

GLEAM continues to improve its performance in providing data both temporally and spatially; even now there is GLEAM version 3 available. GLEAM v3.3a is a global dataset of land-surface evaporation and root zone soil moisture. The dataset is generated using the Priestley-Taylor equation based on reanalysis surface radiation (ERA-5) and near-surface air temperature (ERA-5), a combination of gauge-based, reanalysis, and satellite-based precipitation (MSWEP v2.2) and satellite-based vegetation optical depth (land parameter retrieval model – LPRM) (Martens *et al.* 2017). GLEAM 3.3a data were selected for this study because this model provided the most complete dataset in terms of spatial extents ( $0.25^\circ \times 0.25^\circ$ ) and continuous temporal coverages (daily) for 39 years (1980–2018). And it provided daily evaporation data, while in a drought analysis, the time-scale used is monthly. Therefore, the daily evaporation data would need to be accumulated first into monthly data.

## METHODS

### SPI development

SPI is a drought index developed by McKee *et al.* (1993) and is one of the most frequently used indices in

drought analysis. SPI is considered to be the simplest index to analyse because it only uses one indicator of drought, namely precipitation, and has a small amount of data in the calculation (Shamshirband *et al.* 2020). Drought analysis with SPI is completed by adding up the rainfall during  $k$  months, then the accumulated rainfall is standardized into a parametric statistical distribution, of which probabilities are converted to the standard normal distribution (McKee *et al.* 1993; Stagge *et al.* 2015). By then, the SPI value can be interpreted statistically, which represents the number of standard deviations from the spatial and temporal accumulated rainfall of the year (Stagge *et al.* 2015).

However, for certain times such as the dry season or summer where the rate of rainfall is minimum, the possibility of rainfall accumulation does not exist (zero precipitation), especially for short periods that occur in between 1 and 3 months. In previous SPI studies that have been reviewed by Stagge *et al.* (2015) to solve the zero precipitation, the SPI value is set based on the historical occurrence (%) of periods with zero precipitation in the following equation:

$$p_{(x)} = p_o + (1 - p_o)F(x_{p>0}, \lambda) \quad (1)$$

where  $p$  represents the probability distributions for accumulated precipitation,  $F(x, \lambda)$  is the parametric univariate distribution functions, and  $x, p_o$  is the historical ratio of periods with zero precipitation.

Nonetheless, this method causes a problem because it provides the maximum SPI value. The average SPI value in the normal distribution should be 0; meanwhile, the value is in between two conditions, 50% is in wet conditions and the other 50% is in dry conditions. In this method, the average SPI value has increased so that the value is above 0 (Stagge *et al.* 2015). Therefore, Stagge *et al.* (2015) in their study provided a solution by making the SPI value maintained for statistical interpretability to be in the condition of zero precipitation based on the 'center of mass'. By using zero precipitation based on the 'center of mass', the average SPI value will always be 0 and will not be skewed under different conditions (dry or wet). The formula used to calculate the probability of

'center of mass' for zero precipitation is shown in the following equation:

$$p(x) = \begin{cases} p_o + (1 - p_o)F(x_{p>0}, \lambda), & x > 0 \\ \frac{n_{p=0} + 1}{2(n + 1)}, & x = 0 \end{cases} \quad (2)$$

where  $n$  is the total number of samples in the reference period,  $p$  and  $F(x, \lambda)$  are the probability distribution and the parametric univariate distribution functions for samples that match parameter  $\lambda$  with detectable precipitation accumulation.

After all the probability value has been calculated, the distribution of the SPI value can then be computed. The SPI values require selecting an appropriate parametric probability distribution to convert climate water balance accumulation into standard normal distribution. The selection of an incorrect distribution can cause a fairly high bias in the index value, which results in the value being inaccurate (Stagge *et al.* 2015; Monish & Rehana 2020). The distributions for SPI include normal, log-normal, logistics, log-logistics, Gamma, Gumbel, and Weibull. With extensive statistical testing and relative comparisons such as Kolmogorov-Smirnov (KS), Anderson-Darling (AD), and Shapiro-Wilk, Stagge *et al.* (2015) recommend the gamma distribution to be used for calculating the SPI. The percentage of rejection of the gamma distribution from the results of these tests is the lowest (near to 5%) compared with other distributions so that the gamma distribution becomes the most suitable distribution model. The SPI value with the gamma distribution can be calculated using the following equation:

$$f(x) = \frac{1}{\alpha^\beta \Gamma(\beta)} x^{\beta-1} e^{-\frac{x}{\alpha}}, \quad x > 0 \quad (3)$$

where

$$\Gamma(c) = \int_0^\infty e^{-x} x^{c-1} dx \quad (4)$$

## SPEI development

Different from the SPI analysis, the SPEI analysis is based on the accumulation for  $k$  months and employs the value of the reduction of rainfall with potential evapotranspiration (PET) (Stagge *et al.* 2015). After the accumulation of rainfall minus evapotranspiration is converted into probability, it is then converted into a standard normal distribution to determine the final drought index value. Furthermore, the probability distribution for SPEI requires a location parameter because the climate water balance is not limited by a zero value and can still be analysed, even though the value is negative when the PET value is greater than rainfall. The distributions for SPEI include normal, general logistics, generalized extreme value (GEV), and Pearson Type III distribution (Stagge *et al.* 2015). Stagge *et al.* (2015) suggest to use the GEV distribution when calculating the SPEI after doing some statistical testing such as KS, AD, and Shapiro-Wilk. The suggestion is given because the percentage of rejection of the GEV distribution is the lowest compared with other distributions from the results of these tests so that the GEV distribution becomes the most suitable distribution model, especially for uncertain climatic conditions.

To develop a drought index based on SPEI, it is necessary to ensure that the quality of the precipitation and evaporation data use is complete. SPEI uses the difference between monthly precipitation and PET. After PET is obtained, then the climate water balance for the  $i$ th month ( $D_i$ ) can be calculated by reducing the value of precipitation for the  $i$ th month ( $P_i$ ) with evaporation potential for the  $i$ th month ( $PET_i$ ) as in the following equation:

$$D_i = P_i - PET_i \quad (5)$$

SPEI is standardization based on the GEV distribution. With the GEV distribution, the observed variable will be limited to observing only the maximum or minimum value, which is independent and identically distributed. The probability density function  $f(x)$  of the GEV distribution

is shown in the following equation:

$$f_{(x)} = \begin{cases} \left(\frac{1}{\sigma}\right) \left[ (1 + \xi z(x))^{-\frac{1}{\xi}} \right]^{\xi+1} e^{-\left[ (1 + \xi z(x))^{-\frac{1}{\xi}} \right]}, & \xi \neq 0, 1 + \xi z(x) > 0 \\ \left(\frac{1}{\sigma}\right) e^{-z(x) - e^{-z(x)}}, & \xi = 0, -\infty < x < \infty \end{cases} \quad (6)$$

where

$$Z_{(x)} = \frac{x - \mu}{\sigma} \quad (7)$$

$\mu$ ,  $\sigma$ , and  $\xi$  are parameters of location, scale, and shape, respectively, that have been estimated using the maximum probability. The cumulative GEV distribution function  $F(x)$  can be calculated in the following equation:

$$F_{(x)} = e^{-t(x)} \quad (8)$$

where

$$t_{(x)} = \begin{cases} \left( 1 + \xi \left( \frac{x - \mu}{\sigma} \right) \right)^{-\frac{1}{\xi}}, & \xi \neq 0 \\ e^{-(x - \mu)/\sigma}, & \xi = 0 \end{cases} \quad (9)$$

### Drought classification

The drought index is the main variable for assessing the effects of drought and for determining variations in drought characteristics such as duration, intensity, and severity. In this study, the drought analysis will be calculated on a different scale from 1 to 12 months. Based on SPEI calculations as suggested in McKee *et al.* (1993), drought can be classified into seven categories as listed in Table 1.

SPEI is a standardized variable, and it can be compared with other SPEI values over time and space. Drought occurs when the SPEI value is consistently negative and reaches drought intensity with an SPEI value of  $-1$  or less, and the drought will end if the SPEI value becomes positive. Drought can also be classified based on the frequency of occurrence according to WMO (2012), drought is divided into four categories as listed in Table 2.

47

**Table 1** | Drought classification based on SPEI value (McKee *et al.* 1993)

SPEI value	Condition	Class
$\geq 2$	Extremely wet	1
1.5 s/d 1.99	Wet	2
1.00 s/d 1.49	Moderately wet	3
0.99 s/d -0.99	Normal	4
-1.00 s/d -1.49	Moderately dry	5
-1.50 s/d -1.99	Dry	6
$\leq -2$	Extremely dry	7

19

**Table 2** | Drought classification based on the frequency of occurrence (WMO 2012)

Drought category	SPEI value	Number of times in 100 years	Severity of event
Moderate dryness	-1 s/d -1.49	10	1 in 10 years
Severe dryness	-1.5 s/d -1.99	5	1 in 20 years
Extreme dryness	$\leq -2$	2.5	1 in 50 years

## RESULTS AND DISCUSSION

### The goodness of fit statistics

To prove that the distribution recommended by Stagge *et al.* (2015) is valid and fits with the spatial conditions of Java Island, it is necessary to evaluate the suitability of the distribution known as the goodness of fit (GOF) statistics. The GOF is conducted to test the fit between the observed results (empirical distribution) and the expected results (theoretical distribution). The main purpose of the GOF is to find out whether the resulting data most likely come from a null distribution. The null distribution is when the tested null hypothesis is true on the statistical test probability distribution. The null hypothesis used in this case states that the theoretical distribution (namely data from the model: gamma distribution for SPI and GEV distribution for SPEI) and the empirical distribution (observational data) come from the same population, then the significance rate used is 95%. The GOF to be evaluated uses three different parameters, namely the KS test, the AD test, and the Cramér-von Mises (CVM) statistical test.

The KS, AD, and the CVM tests are non-parametric suitability tests for two independent samples that are often used to determine whether the null hypothesis is rejected or accepted. The KS test is widely used in statistical testing for two distribution equations because the procedure is relatively simple. This test measures the distance between the two distributions, defined as the difference in the maximum value (the cumulative distribution function minus the empirical distribution function) that may occur (Wijekularathna *et al.* 2019). The greater Kolmogorov distance will decrease the  $p$ -value, and the null hypothesis ( $H_0$ ) is rejected. Hence, the higher  $p$ -value indicates that the covariate distributions of the two matched samples are not statistically different from each other.

Meanwhile, the AD test is a non-parametric statistical procedure that arises from a general distribution function and is not determined by the empirical distribution function (Wijekularathna *et al.* 2019). The hypothesis of this test is that the population of two or more data classes drawn is identical. Each class must be an independent random sample from a population. Basically, the statistical test is carried out by a double sum of integrated squared differences between the empirical distribution functions of the collected sample and the individual samples (Wijekularathna *et al.* 2019).

Then, the CVM test can be measured by the square of the difference between the empirical distribution and the hypothetical cumulative density function (Wijekularathna *et al.* 2019). CVM statistics use half-point correction, taking into account all ordered data points. The distribution of  $F$  under  $H_0$  is uniform at  $(0,1)$ , thus simplifying the calculation. This test takes the dataset as its argument and returns the  $p$ -value so that  $H_0$  will be rejected if the  $p$ -value is  $<0.05$ .

This study investigates time-series datasets (SPI and SPEI) from grid points over Java with different timescales (1–12 months) whether the observation datasets are able to be modelled reasonably by gamma and GEV distributions, respectively. In addition, the datasets are also classified into 12 different months (January–December) separately. Tables 3 and 4 present the number of the grid points (in %) statistically accepted for different timescales and months. In the grid points, the data generated from the theoretical distribution match the empirical distribution data.

In Table 3, the percentage of acceptance rates for the gamma distribution using the KS, AD, and CVM tests

shows values that are not much different from one another. During 12 months (January–December) with varying scales of time, the percentage value tended to fluctuate but was not significant. In general, the number of the grid points statistically accepted is above 93% of Java for all 12 months and different timescales. This indicated that the gamma distribution is suitable to model rainfall amount in Java for different seasons and a variety of timescales.

Similar to the gamma distribution, the GEV distribution is also fit to the observation datasets (rainfall minus evapotranspiration), which is used for the SPEI model. The percentage of acceptance rate among all grid points in Java shows a very high rate. In fact, Table 4 shows that the percentage of acceptance rate tends to be better and more stable than the gamma distribution for the SPI model. This result is supported by Stagge *et al.* (2015), which explains that the level of acceptance of SPEI distribution is higher than SPI, which is caused by the characteristics of the climate water balance that SPEI has, and is not limited by zero precipitation. The parametric distribution is therefore easier to adjust to the distribution of the accumulated climate water balance, which results in the distribution for SPEI having a higher acceptance rate.

### Monthly temporal variation of SPI and SPEI values

Two grid points are selected as the samples of different geographic locations to explain the monthly temporal variation of SPI and SPEI values during the period of 1980–2018. The first grid point is located in Indramayu with the Point ID-30. This location is characterized as a coastal low land area with an elevation of 1 m from mean sea water level (MSWL). This region has an average monthly temperature ranging between 26 and 28.5 °C, a minimum temperature fluctuating from 23.8 to 25.1 °C, a maximum temperature varying from 28.9 to 32.9 °C, and a mean monthly rainfall ranging from 13 to 283 mm. The second grid point is situated in Garut with the Point ID-155. In contrast to the Point ID-30, this place is categorized as a mountainous region with an elevation of 993 m from MSWL. Like other typical mountainous climate regions, this place has lower temperatures but higher amounts of rainfall. This region has an average temperature ranging between 20.2 and 21.3 °C, a minimum temperature of 16.6–18.9 °C, a maximum temperature of

**Table 3** | Percentage of spatial grids in Java for which the Gamma Distribution is accepted to model rainfall amounts (significance level 95%) for 12 months (January–December), different timescales (1–12 months) using three different statistical tests, namely KS, AD, and CVM

		15 Jan	Feb	Mar	Apr	May	Jun	Jul	Aug	Sep	Oct	Nov	Dec
t1	KS	96.62	99.25	96.99	96.24	95.86	98.87	98.12	98.50	99.25	96.62	94.74	98.50
	AD	96.24	98.50	96.99	95.86	96.24	98.50	98.12	98.87	98.50	98.87	95.86	98.87
	CVM	96.62	98.50	95.86	93.23	96.24	98.87	96.99	97.37	98.87	96.62	94.36	98.50
t2	KS	97.74	97.74	97.37	98.85	96.99	98.87	99.25	98.87	98.50	95.86	94.36	96.24
	AD	98.50	98.87	97.74	98.09	97.37	99.25	99.25	99.25	98.87	96.24	94.74	95.49
	CVM	97.74	98.12	98.12	97.71	96.62	98.87	98.50	98.12	98.87	95.11	93.98	95.11
t3	KS	98.50	96.99	97.74	98.87	98.12	98.87	98.50	98.87	97.74	98.50	97.37	98.12
	AD	98.87	98.50	98.50	98.50	98.50	97.74	99.25	99.25	99.62	98.87	98.12	98.87
	CVM	97.74	97.37	98.12	98.12	98.12	97.37	99.25	99.25	98.87	98.50	97.74	96.99
t4	KS	97.74	98.50	97.74	98.50	97.74	98.50	98.87	98.50	99.25	97.37	96.24	97.74
	AD	97.74	98.50	98.87	98.50	98.87	98.12	98.12	98.87	99.25	97.37	96.99	98.12
	CVM	96.62	98.50	98.50	97.37	98.12	98.50	97.74	98.50	99.25	96.99	96.99	96.62
t5	KS	96.99	97.37	98.50	98.50	99.25	98.50	97.37	99.62	99.62	99.25	96.24	97.74
	AD	98.12	98.50	99.25	98.87	98.87	98.87	98.87	99.25	99.62	98.87	98.12	98.12
	CVM	96.99	97.37	98.87	98.50	98.50	98.87	97.37	99.25	99.62	99.25	98.50	98.12
t6	KS	98.85	98.87	98.50	98.12	97.74	98.87	98.50	98.87	99.25	98.87	97.37	97.74
	AD	99.24	98.50	98.50	98.50	98.87	99.25	99.25	99.62	99.62	98.50	97.37	98.87
	CVM	99.24	98.12	98.12	97.74	98.50	99.25	98.50	99.62	99.25	98.50	97.74	97.74
t7	KS	98.87	98.87	99.62	98.50	98.50	98.50	97.74	97.74	98.12	98.50	99.62	98.50
	AD	98.87	99.25	99.62	98.50	98.50	98.50	98.50	98.12	98.87	99.62	99.62	99.25
	CVM	98.50	98.87	98.87	98.12	98.50	98.87	97.37	98.50	98.50	98.87	98.87	97.74
t8	KS	99.25	98.87	99.25	98.87	97.37	98.50	98.87	98.50	98.50	98.50	98.50	96.99
	AD	99.25	99.25	98.12	99.25	98.12	99.25	98.87	98.50	99.25	99.25	96.99	98.12
	CVM	98.50	99.25	98.12	99.25	97.74	98.87	98.50	98.12	98.50	98.50	97.37	97.74
t9	KS	97.74	97.37	99.62	98.50	98.87	98.12	99.25	98.47	98.50	98.12	99.25	97.74
	AD	98.50	98.12	99.62	98.87	99.25	98.50	99.62	99.62	98.12	98.87	98.50	98.50
	CVM	98.12	97.74	98.87	98.87	99.25	98.50	99.25	99.62	98.50	98.12	98.12	98.12
t10	KS	98.50	98.50	98.50	99.25	98.87	98.12	98.87	97.37	98.12	99.25	98.50	97.71
	AD	99.62	99.25	98.50	98.87	99.25	98.50	99.25	98.50	98.87	99.25	98.50	98.85
	CVM	98.50	98.50	98.50	98.87	99.25	98.12	98.87	98.12	98.50	98.12	98.50	98.85
t11	KS	98.87	98.87	98.87	97.74	99.25	98.50	97.37	98.50	97.74	98.87	96.99	99.62
	AD	99.62	98.50	98.87	98.50	99.25	98.87	98.50	98.12	99.25	98.50	98.50	99.62
	CVM	98.50	98.50	97.74	98.87	98.50	98.12	97.74	98.12	99.25	97.74	99.25	98.87
t12	KS	98.12	98.50	98.87	98.50	99.25	98.87	98.87	98.50	98.87	99.25	98.87	98.12
	AD	98.87	99.25	99.25	98.87	99.25	98.50	99.25	99.62	99.62	98.87	98.87	99.25
	CVM	98.87	98.50	97.74	98.87	99.25	98.12	98.87	98.50	98.12	99.25	99.25	98.87

24.7–25.7 °C, and a mean monthly rainfall ranging from 73 to 517 mm.

In general, drought indices derived by the SPI method present systematically lower than the SPEI approach, particularly for the upper thresholds from –1 to –2 as shown in Figure 4. This means drought severity generated by SPI reveals systematically higher other than SPEI for a given month. Figure 63 presents a monthly temporal variation of drought indices for

both SPI and SPEI during the period of 1980–2018. The blue lines show the SPI values, while the red lines represent the SPEI values. From the figure, it can be seen that the drought indices based on the SPI analyses dominate the lowest margin. The lowest SPI value was around –2.964, while SPEI was only –2.529 for the Point ID-30. Similarly, for the Point ID-155, the lowest SPI value was –3, while SPEI was –2.69. Even at the 175th month, both locations

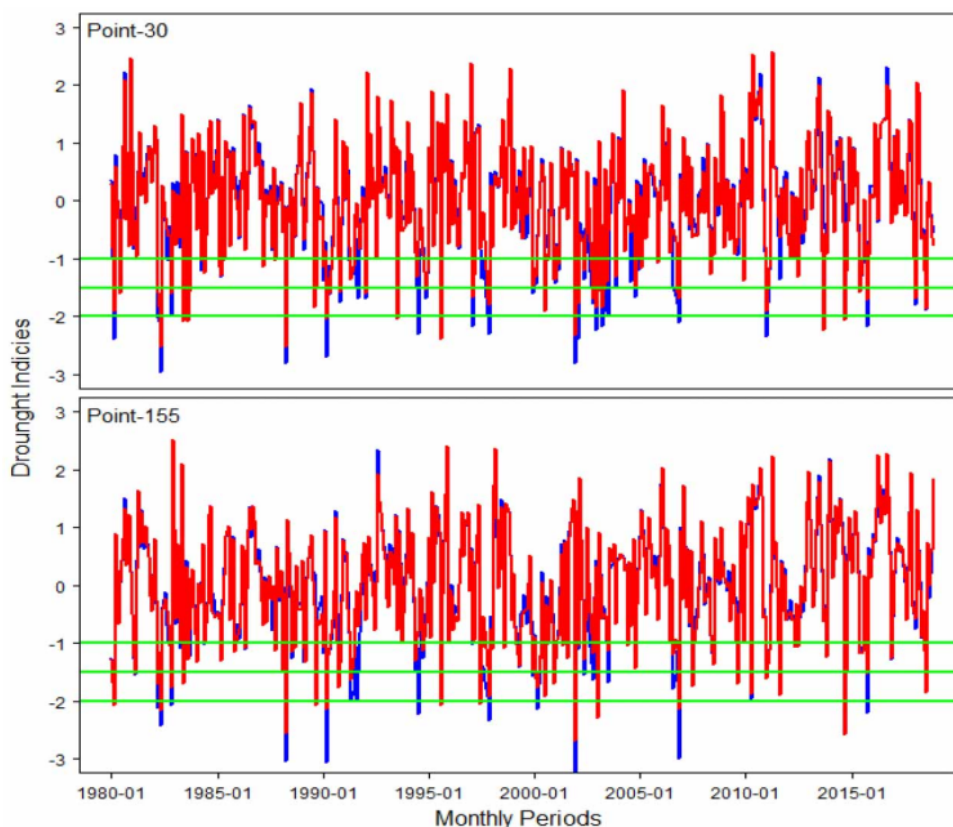
**Table 4** | Percentage of spatial grids in Java for which the GEV distribution is accepted to model rainfall minus evapotranspiration amounts (significance level 95%) for 12 months (January–December), different timescales (1–12 months) using three different statistical tests, namely KS, AD, and CVM

		15 Jan	Feb	Mar	Apr	May	Jun	Jul	Aug	Sep	Oct	Nov	Dec
t1	KS	99.07	99.53	97.55	99.51	99.07	99.53	99.07	98.53	97.58	97.66	99.05	97.66
	AD	99.07	99.53	99.02	99.51	98.60	99.07	99.53	99.51	99.03	99.53	99.53	98.60
	CVM	98.60	99.53	98.04	99.51	98.60	99.07	97.20	98.53	98.07	98.60	99.53	97.66
t2	KS	98.60	99.02	99.52	99.50	98.56	99.07	99.07	98.59	98.01	99.07	98.58	99.06
	AD	99.07	99.51	99.05	99.50	98.09	99.07	99.07	98.12	98.51	99.07	99.06	98.58
	CVM	99.07	99.02	99.05	98.51	98.56	99.53	97.66	97.18	98.01	98.60	98.58	98.58
t3	KS	99.51	98.58	98.57	99.52	99.01	98.60	99.07	99.07	99.53	98.60	97.66	99.02
	AD	99.51	99.06	98.57	99.52	99.50	99.07	98.13	99.53	99.53	99.53	99.07	99.51
	CVM	99.51	99.06	98.10	99.52	99.50	99.07	98.13	99.07	99.53	99.53	99.07	99.02
t4	KS	99.47	98.58	99.03	99.01	95.52	99.04	99.07	99.07	99.53	98.60	99.07	98.60
	AD	98.95	99.53	99.51	99.51	98.01	99.04	99.53	99.07	99.53	99.53	99.07	99.53
	CVM	98.95	99.05	99.03	99.01	97.01	99.04	99.07	98.60	99.53	98.60	98.13	99.53
t5	KS	99.03	99.48	97.96	99.01	94.95	97.66	98.13	97.66	98.60	99.07	98.13	98.60
	AD	99.52	99.48	99.49	99.01	96.97	99.07	98.60	99.53	99.07	99.53	99.07	99.07
	CVM	99.52	98.43	99.49	99.01	96.97	99.07	98.13	98.13	99.53	99.53	99.07	98.60
t6	KS	97.62	99.52	98.77	99.44	99.03	98.57	98.13	99.53	98.60	98.60	99.53	99.53
	AD	98.57	99.52	98.77	98.89	99.51	98.57	98.60	99.53	99.53	99.07	99.53	99.53
	CVM	98.10	98.56	98.16	98.89	99.03	98.57	99.07	99.53	99.07	98.60	98.13	99.53
t7	KS	98.56	99.53	97.08	99.38	99.48	98.56	97.20	97.66	99.07	98.60	99.53	99.06
	AD	98.56	99.53	97.66	99.38	99.48	99.04	96.73	99.53	99.53	99.53	99.07	99.06
	CVM	98.08	99.53	98.25	99.38	99.48	98.56	96.26	98.13	99.07	99.53	99.07	99.06
t8	KS	99.07	99.52	97.84	95.93	99.48	97.46	99.03	98.59	96.73	98.13	99.07	98.13
	AD	99.53	99.05	99.46	98.84	99.48	99.49	99.52	99.06	97.66	99.07	99.53	99.07
	CVM	99.07	99.05	98.38	98.84	99.48	99.49	99.52	98.59	98.13	99.07	99.53	99.07
t9	KS	98.60	98.60	97.40	98.36	98.96	98.47	98.00	99.02	97.65	99.53	99.53	98.13
	AD	99.53	98.60	97.92	98.36	99.48	99.49	98.50	99.51	99.53	99.53	99.53	99.07
	CVM	99.53	99.07	97.92	97.81	99.48	98.98	98.50	98.04	99.06	99.53	99.53	98.60
t10	KS	99.07	99.07	98.55	98.40	97.50	97.97	99.02	98.97	99.51	97.64	99.07	99.07
	AD	99.53	98.60	98.07	98.93	98.00	98.48	99.02	98.97	99.01	98.11	99.53	99.53
	CVM	99.07	98.60	98.07	99.47	98.00	97.97	98.53	98.46	99.51	97.17	99.07	98.60
t11	KS	97.66	99.07	98.58	99.02	98.97	98.47	99.50	98.50	96.94	99.00	98.04	99.53
	AD	99.07	99.53	99.53	99.51	98.97	98.98	99.01	99.00	98.98	98.01	99.02	99.53
	CVM	98.60	99.53	99.05	99.51	98.97	98.98	99.50	98.50	98.98	98.01	99.02	99.06
t12	KS	98.60	99.51	98.60	98.60	99.52	98.47	99.49	98.49	97.99	98.97	98.99	98.52
	AD	99.07	99.51	99.07	98.60	99.52	98.98	99.49	98.99	98.99	98.97	98.49	99.51
	CVM	99.07	99.51	99.07	98.60	99.52	98.47	98.99	98.99	98.49	98.97	98.99	98.52

showed a significant difference between the SPI and SPEI values. The SPI value at Point ID-30 was  $-2.289$ , while the SPEI value was  $-0.7$  and the SPI and SPEI values at Point ID-155 were  $-2.217$  and  $-0.79$ , respectively.

Apart from showing a lower value, SPI also detected the number of dry months (months of drought) more than SPEI. SPI detected 78 out of 468 months of drought, while SPEI detected 73 months on Point ID-30 (Indramayu). Whereas

from the detection results, the drought incidence based on SPI/SPEI has a match with the actual events from 2003 to 2018 that were recorded by DIBI in June 2003, July 2003, August 2004, November 2006, August 2011, and July 2018. Interestingly, SPI and SPEI detected almost the same number of drought at Point ID-155 (Garut) of 83 and 82 months, respectively. Different from Indramayu, Garut succeeded in detecting more drought events similar to that of



**Figure 4** | The comparison of SPI-1 and SPEI-1 at Point ID-30 (Indramayu) and Point ID-155 (Garut). The vertical axes represent drought indices for SPI (blue lines) and SPEI (red lines). The horizontal axes define months (January 1980–December 2018). Please refer to the online version of this paper to see this figure in colour: doi:10.2166/wcc.2021.022.

the actual drought in July 2003, October 2004, August 2006, November 2006, June 2008, July 2008, August 2011, and July 2018. This indicates that the SPI approach yields a conservative estimation compared with the SPEI model for both locations. However, in the mountainous region (Garut), SPI and SPEI present quite similar behaviour due to low temperature and high total rainfall.

Nevertheless, temporal variations of both indices exhibit similar patterns. This means that there is a strong correlation between two drought indices. Based on Figure 4, it can be seen that there are several patterns that show one of the lines is far from each other. This pattern difference mostly occurs from April to September (dry season). So, when the dry season comes, the temperature would increase and cause the evaporation to increase, while the rainfall

decreases. With the increase of evaporation rate, the availability of water would decrease which eventually causes an area to become drier. This, in turn, causes SPEI to have a lower value than SPI during the dry season and indicates that temperature may influence the correlation between SPI and SPEI.

These results are supported by a study conducted by Zhang *et al.* (2019). From their research, it was concluded that the frequency of drought would increase, while the correlation decreases with the increased value in temperature. In their research, the frequency of drought decreased from the highest to the lowest margin in summer, autumn, spring, and winter, respectively. However, the results of our research are contradictory to those in Gurrupu *et al.* (2014), as the study concluded that the correlation between

SPI and SPEI was weaker in winter and relatively stronger in summer, autumn, and spring. The correlation between the two analyses during winter was weaker but positive, whereas the correlation in April was weaker and negative, which was probably due to the increased river flow from rapid snowmelt.

The difference in results may be due to different conditions in the study area. In Java, there are only two seasons and there is no snow, so during the dry season, when the temperature increases, the area will become drier. It is different from the study reported in the research by Gurrapu *et al.* (2014), where there is snow in the research location so that with the increasing temperature, the water availability in the area increases due to snowmelt.

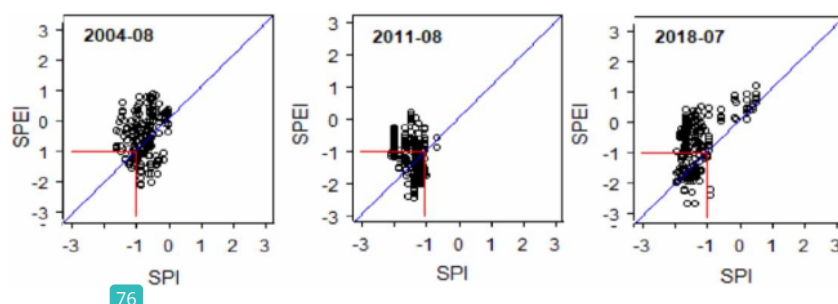
### Comparison of SPI and SPEI values with historical droughts

Three historical drought events were selected as samples to evaluate how reliable SPI/SPEI methods estimate drought events. During the 16 years of recording drought incidents contained in DIBI, the number of drought occurrences that occurred at one time varied greatly. The varying number of drought events can be due to the location of Java Island, which is between two oceans (Pacific and Indian) and two continents (Asia and Australia), which causes a natural phenomenon, namely El Nino. The level of strength of El Nino can be determined through the Oceanic Nino Index (ONI), which is the standard used for NOAA. ONI classifies El Nino into four levels based on sea surface temperature, including weak (0.5–0.9), moderate

(1–1.4), strong (1.5–1.9), and very strong ( $\geq 2$ ). DIBI recorded that the highest number of droughts in Java occurred in August 2004, August 2011, and July 2018, where El Nino with a weak category was also hitting Java.

Therefore, the three drought events that occurred in different years would be discussed. This would later be compared with the historical droughts recorded by DIBI. One point to consider is when the drought event in DIBI is recorded at the beginning of the month, the drought data recorded in the previous month will be used, while those recorded at the end of the month will use the drought data for that particular month. The results of drought analysis in August 2008, August 2011, and July 2018 are as shown in Figure 5.

Spatial distributions among 144 cities/regencies of drought occurrences in August 2004 were under-estimated by both SPEI and SPI methods. Based on Figure 5, the drought events occurred when the dots (cities/regencies) were located below the red lines or the SPI and SPEI values were less than or equal to  $-1$ . Historical drought hazards in August 2004 recorded that 42 cities were suffering drought hazards, including four cities in Banten, 15 cities in West Java, 18 cities in Central Java, one city in Yogyakarta, and four cities in East Java provinces. However, the SPI method detected 25 cities that were facing drought disasters covering three cities in Banten province, five cities in West Java province, 12 cities in Central Java province, and five cities in East Java province. Meanwhile, SPEI methods were applied to 22 cities suffering droughts, including three cities in Banten province, six cities in West Java province, 12 cities in Central Java province, and one city in Yogyakarta province.



**Figure 5** | The spatial distributions of drought events based on SPI and SPEI values for all grid points and for selected drought occurrences (August 2004, August 2011, and July 2018). The vertical axes are drought indices generated by SPEI and the horizontal axes are drought index produced by SPI. Please refer to the online version of this paper to see this figure in colour. doi:10.2166/wcc.2021.022.

In contrast to August 2004, both SPI and SPEI methods overestimate a number of cities/regencies suffering drought hazard. While the factual drought regions recorded by DIBI were distributed across 39 cities/regencies, the SPEI method predicted 46 cities/regencies hit by drought, and the SPI method estimated 82 cities/regencies. This indicates that SPEI performs better other than SPI. A number of 39 factual drought cities/regencies were distributed in four cities in Banten, 17 cities in West Java, 11 cities in Central Java, and seven cities in East Java provinces. In total, 46 drought cities/regencies estimated by SPEI include six cities in Banten, one city in DKI Jakarta, 18 cities in West Java, 16 cities in Central Java, one city in DI Yogyakarta, and four cities in East Java provinces. In total, 82 drought cities calculated by the SPI model are six cities in Banten, one city in DKI Jakarta, 20 cities in West Java, 24 cities in Central Java, four cities in Yogyakarta, and 27 cities in East Java provinces. SPI performs worst in East Java, while SPEI performs worst in Central Java.

Last, in July 2018, DIBI recorded 62 cities experiencing droughts covering six cities in Banten, 17 cities in West Java, 21 cities in Central Java, two cities in Yogyakarta, and 16 cities in East Java. Interestingly, in this particular month, SPI and SPEI detected the same number of droughts and cities. Both indices successfully detected 70 cities covering six cities in Banten, one city in Jakarta, 20 cities in West Java, 22 cities in Central Java, three cities in Yogyakarta, and 18 cities in East Java.

From these results, it can be seen that on average, SPI usually detects more drought events than SPEI. Even in August 2011, the difference between the two indices was very significant in detecting the number of drought events. To better understand how the characteristics of SPI and SPEI in detecting drought, the following table presents a recapitulation of drought events that occurred in cities or districts. The recapitulation contains the total drought incidents based on DIBI, SPI, and SPEI (Table 5).

The SPI provides an overestimate of events when detecting drought that was very much different from the SPEI and actual drought occurrences. Even though, in several cities, SPEI detected a greater drought event than SPI, the difference in numbers given by the SPEI was relatively low and did not differ much from that of the SPI. This is evidenced by the number of drought events from 2003 to 2018 in 16

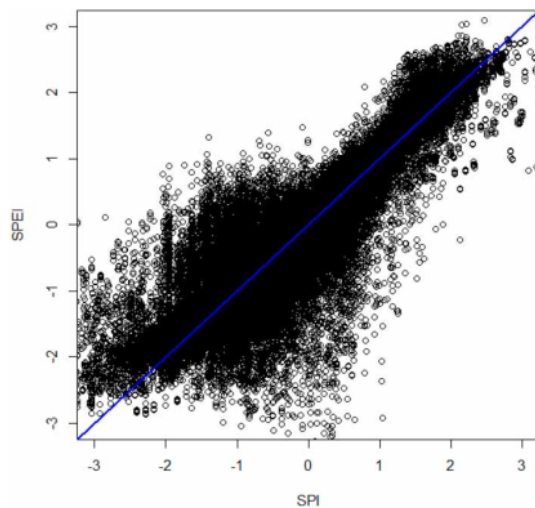
**Table 5** | Recapitulation of drought events from 2003 to 2018 based on DIBI, SPI, and SPEI

City	Total of drought events		
	DIBI	SPI	SPEI
Ponorogo	50	213	80
Bojonegoro	48	200	88
Wonogiri	45	97	102
Nganjuk	40	75	50
Sragen	38	259	120
Kuningan	34	176	52
Semarang	32	63	70
Situbondo	31	176	52
Ciamis	30	38	53
Cirebon	29	75	50
Garut	29	105	86
Tasikmalaya	29	101	48
Bandung	28	45	145
Serang	27	127	94
Indramayu	26	38	28
Sumedang	26	259	120

cities, which are presented in Table 5. When compared with DIBI, the highest estimate given by the SPI for the Sragen district was 221 events, while the lowest estimate was for the Ciamis district with as many as eight drought events. The highest estimate given by SPEI occurred in Bandung city with a total drought of 117 events, then the lowest estimate was two events that occurred in the Indramayu city. This indicates that SPI is very conservative and SPEI is more moderate in estimating drought events.

#### Effect of different timescales on similarity of the SPI and SPEI

A scatter plot was used for analysing between SPI and SPEI for determining how closely both indices are related. There was a significant positive correlation between SPI and SPEI, which is seen from the tendency of the data to gather around the diagonal line. The results of the correlation analysis are set out in Figure 6. The SPI and SPEI can actually be used to calculate the drought index for a variety of different timescales. In this study, a different timescale will be used ranging from 1 to 12 months. Most studies have only used

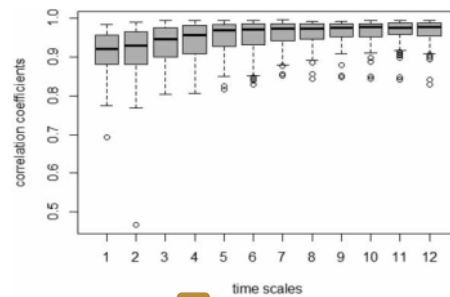


**Figure 6** | Scatter plot of SPI and SPEI values for all grid points and all timescales (1–12 months).

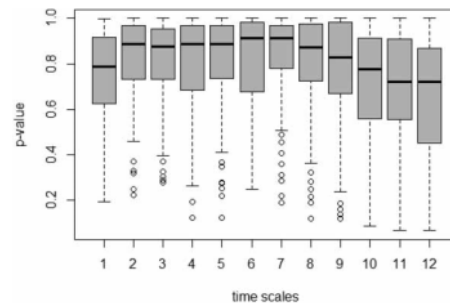
fewer timescales such as 1, 3, 6, and 12 months, while this study has the advantage of being more detailed in order to see the correlation between SPI and SPEI.

To determine more detail about the relationship between SPI and SPEI which was on different timescales, the correlation coefficient and the KS test were used. The difference in SPI and SPEI values may be due to differences in data variables used as input to calculate the drought index. For example, in the event of the same drought, the SPI index may show a value of 1, while the SPEI may show a value of 3. This is possible because the SPI only calculates drought events based on the rainfall rate, while the SPEI identifies drought events not only based on the rainfall rate but also the evapotranspiration of the region. This view is supported by Gurrapu *et al.* (2014) who write that the differences in the variables used as input data in analysing drought will affect the value of the drought index.

The correlation between SPI and SPEI is consistently increasing along with the longer the timescale used. It can be seen from the box plot in Figure 7 that the value of the correlation coefficient is above 0.9 for all timescales. This showed that the relationship between SPI and SPEI is strong. The 1- to 6-month timescale tends to have a higher significant increase in the correlation coefficient value than the 7- to 12-month timescale, which has a slight



**Figure 7** | Boxplot of the Pearson correlation coefficient between SPI and SPEI values for all grid points during the period of 1980–2018 at different timescales (from monthly to yearly).



**Figure 8** | Boxplot of KS test ( $p$ -value with significance level 5%) between SPI and SPEI values for all grid points during the period of 1980–2018 at different timescales (from monthly to yearly).

increase in the value of the correlation coefficient. Then, in Figure 8 that depicts the results of the KS Test, the  $p$ -value in the 1- to 2-month timescale tends to have a significant increase and then becomes stable up to the 7-month timescale. However, in the 8-month timescale, the  $p$ -value continues to decline up to the 12-month timescale. This indicates that the timescale for the long term is better than the short to medium term.

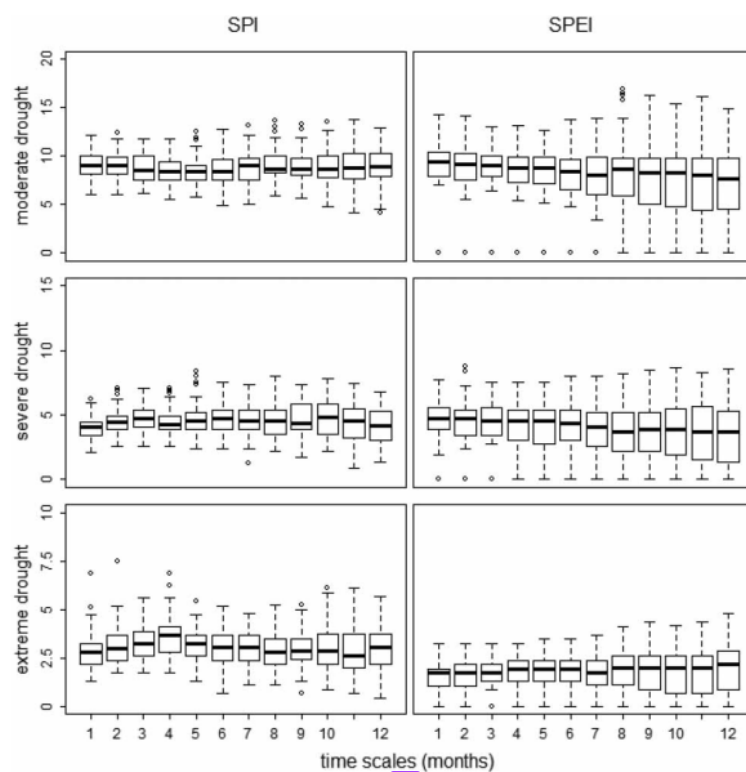
For the drought index, especially from the SPI and SPEI analyses, the use of different timescales will result in different implications from one another (Nam *et al.* 2015). Thus, those calculations of drought with different timescales are often used as information to determine water resources management policies in the short, medium, and long term. The timescales that are often used to measure drought

values are 1-, 3-, 6-, and 12-month timescales. The drought index with a 1-month timescale is included in the short-term period, the 3- and 6-month timescale is included in the medium-term period, and the 12-month timescale is included in the long-term period (Nam *et al.* 2015). The 1-month timescale is more suitable for identifying soil moisture conditions, the 3-month timescale is better for predicting seasonal rain conditions, and the 6- and 12-month timescales are more appropriate for determining the impact of drought on water availability in rivers, ponds, or reservoirs.

### Drought frequency value

In addition to the SPI and SPEI values, this research also discussed the frequency of drought events. Drought events are categorized into three, namely moderate drought

which is included in class 5, severe drought which is included in class 6, and extreme drought which belongs to class 7. The frequency of moderate drought is the percentage of the number of events that have the SPI/SPEI value of  $-1.00$  to  $-1.49$ , which is then divided by the total drought events (which have the SPI/SPEI value of  $-1.00$  to  $-3.00$ ). The frequency of severe drought is the percentage of the number of events that have the SPI/SPEI value of  $-1.50$  to  $-1.99$ , which is later divided by the total number of drought events. The frequency of extreme drought is the percentage of the number of events that have the SPI/SPEI value of  $-2.00$  to  $-3.00$ , which is then divided by the total drought events. As for the frequency value for moderate, severe, and extreme droughts, it is based on the SPI with a timescale of 1–12 months. The percentage of moderate, severe, and extreme drought frequencies based on the SPI and SPEI for all timescales can be seen in Figure 9.



**Figure 9** | Boxplot of frequencies (the number of events) of moderate, severe, and extreme droughts (%) for both SPI and SPEI for all grid points during the period of 1980–2018 at different timescales (from monthly to 12 months).

The frequency rate for SPI will fluctuate more, as the severity of drought increases with the timescale used, whereas for the SPEI with the timescale used, the more severe the level of drought, the more stable the frequency rate. The results of moderate, severe, and extreme droughts are presented in Figure 9. It can be seen that for moderate drought, the highest frequency based on the SPI was 12.18%, while based on the SPEI was 14.32%. Then, the highest frequency, for severe drought, based on the SPI was 6.2%, while based on the SPEI was 7.69%. Meanwhile, for extreme drought, the highest frequency based on the SPI was 6.84%, while based on the SPEI was 3.21%. SPEI has a higher frequency for moderate and severe droughts than SPI, while for extreme drought, the frequency generated by SPI is higher. This indicates that in detecting drought, SPI assesses drought at a more severe level than SPEI.

From the above explanation, it can be concluded that in general the frequency rate for the SPEI is much more stable than that for the SPI, and the drought frequency produced by the SPEI is higher than that by the SPI. With regard to two of the three types of drought frequency, moderate and severe, the SPEI recorded a drought frequency value higher than the SPI. This is due to the existence of the evapotranspiration variable in the SPEI. This feature allows identifying drought events even when the rainfall is not available, so that the index can still be used to capture drought events and calculate the frequency of drought events. Meanwhile, the SPI's extreme drought frequency is higher than that of the SPEI's. Furthermore, the pattern shown for the change in the frequency value against time caused by the SPI and SPEI marks one thing in common, namely the possibility of fluctuations for all types of drought. However, overall the SPEI's drought frequency is more stable than that of the SPI's.

These results are supported by research conducted by Tirivarombo *et al.* (2018). The study found that the SPI was superior in capturing extreme drought events compared with the SPEI. The reason is that when identifying drought that only considers the variable of rainfall, the SPI of which input data are only the rainfall variable will be better to identify extreme drought than the SPEI. The results of the correlation analysis between the SPI and SPEI clearly show that rainfall is the main cause of the drought. It should be noted that the existence of PET becomes important at longer timescales since the correlation is stronger.

## CONCLUSIONS

The conclusions drawn from the results and discussions can be explained as follows.

A comparison between the SPI and SPEI values to temporal variation shows that the correlation between the two indices is quite high for all months for the 1-month timescale. However, this correlation has decreased in the dry months (dry season). In almost all months, the SPI and SPEI values have similar margins with no significant difference, and the SPI value is always below the SPEI value. Yet, in the dry months, the SPEI value is far below the SPI value. This indicates that the temperature variable affects the correlation between the SPI and SPEI because during the dry season the evaporation rate increases more rapidly, resulting in a lower SPEI value than in normal conditions.

The SPI is more conservative in detecting drought than the SPEI. This is indicated by the fact that the SPI detects an overestimation compared with the SPEI and historical data on drought events in Indonesia. Besides, the difference in the timescale used in the analysis will affect the correlation between the SPI and SPEI. The correlation between the SPI and SPEI will get stronger as the timescale used increases.

Then for moderate and severe droughts based on the SPEI, the SPEI shows a higher frequency than the SPI, while for extreme drought, the frequency shown by the SPI is higher. This is because when drought takes into account only the rainfall, the SPI that has one indicator in the form of rainfall will be better at identifying extreme drought than SPEI. The results of the correlational analysis between the SPI and SPEI clearly show that rainfall is the main cause of drought. However, evaporation indicators are also important, especially on a longer timescale where their existence affects the correlation between the SPI and SPEI.

By comparing the two indices, it can be seen how the characteristics and correlations between the SPI and SPEI are. Also, we could identify further the influence of precipitation and evaporation parameters in analysing drought in Java Island. Therefore, this research is expected to be one of the sources of information that can help related parties, especially the BMKG in monitoring drought in Indonesia.

## 17 DATA AVAILABILITY STATEMENT

All relevant data are included in the paper or its Supplementary Information.

## REFERENCES

- Blauhut, V. 2020 The triple complexity of drought risk analysis and its visualisation via mapping: a review across scales and sectors. *Earth-Science Reviews* **210**, 103345. <https://doi.org/10.1016/j.earscirev.2020.103345>.
- BPS 2019 *Indonesia's Product, Harvested Area, and Rice Productivity in 2019*. Indonesian Statistics, Jakarta.
- Gebremeskel, G., Tang, Q., Sun, S., Huang, Z., Zhang, X. & Liu, X. 2019 Droughts in East Africa: causes, impacts, and resilience. *Earth-Science Reviews* **193**, 146–161. <https://doi.org/10.1016/j.earscirev.2019.04.015>.
- Ghorbani, M. A., Kazempour, R., Chau, K. W., Shamshirband, S. & Ghazvinei, P. T. 2018 Forecasting pan evaporation with an integrated artificial neural network quantum-behaved particle swarm optimization model: a case study in Talesh, Northern Iran. *Engineering Applications of Computational Fluid Mechanics* **12** (1), 724–737. <https://doi.org/10.1080/19942060.2018.1517052>.
- Gurrapu, S., Chipanshi, A., Sauchyn, D. & Howard, A. 2014 Comparison of the SPI and SPEI on predicting drought conditions and streamflow in the Canadian prairies. In: *28th Conference on Hydrology and the 26th Conference on Climate Variability and Change, 2010*, p. 7.
- Holden, Z. A., Jolly, W. M., Swanson, A., Warren, D. A., Jencso, K., Maneta, M. & Landguth, E. L. 2019 A topographically resolved wildfire danger and drought monitoring system for the conterminous United States. *Bulletin of the American Meteorological Society* **100** (9), 1607–1613. <https://doi.org/10.1175/BAMS-D-18-0178.1>.
- Jati, M. I. H., Suroso & Santoso, P. B. 2019 Prediction of flood areas using the logistic regression method (case study of the provinces Banten, DKI Jakarta, and West Java). *Journal of Physics: Conference Series* **1367** (1), 012087.
- Martens, B., Miralles, D. G., Lievens, H., Fernández-Prieto, D. & Verhoest, N. E. C. 2016 Improving terrestrial evaporation estimates over continental Australia through assimilation of SMOS soil moisture. *International Journal of Applied Earth Observation and Geoinformation* **48**, 146–162. [doi:10.1016/j.jag.2015.09.012](https://doi.org/10.1016/j.jag.2015.09.012).
- Martens, B., Miralles, D. G., Lievens, H., Van Der Schalie, R., De Jeu, R. A. M., Fernández-Prieto, D. & Verhoest, N. E. C. 2017 GLEAM v3: satellite-based land evaporation and root-zone soil moisture. *Geoscientific Model Development* **10** (5), 1903–1925. <https://doi.org/10.5194/gmd-10-1903-2017>.
- McKee, T. B., Doesken, N. J. & Kleist, J. 1993 The relationship of drought frequency and duration to time scales. In *Proceedings of the 8th Conference on Applied Climatology* **17** (22), 179–183.
- Monish, N. T. & Rehana, S. 2020 Suitability of distributions for standard precipitation and evapotranspiration index over meteorologically homogeneous zones of India. *Journal of Earth System Science* **129** (1). <https://doi.org/10.1007/s12040-019-1271-x>.
- Nam, W. H., Hayes, M. J., Svoboda, M. D., Tadesse, T. & Wilhite, D. A. 2015 Drought hazard assessment in the context of climate change for South Korea. *Agricultural Water Management* **160**, 106–117. <https://doi.org/10.1016/j.agwat.2015.06.029>.
- Pang, J., Zhang, H., Xu, Q., Wang, Y., Wang, Y., Zhang, O. & Hao, J. 2020 Hydrological evaluation of open-access precipitation data using SWAT at multiple temporal and spatial scales. *Hydrology and Earth System Sciences* **24** (7), 3603–3626. <https://doi.org/10.5194/hess-24-3603-2020>.
- Peng, J., Dadson, S., Hirpa, F., Dyer, E., Lees, T., Miralles, D. G. & Funk, C. 2020 A pan-African high-resolution drought index dataset. *Earth System Science Data* **12** (1), 753–769. <https://doi.org/10.5194/essd-12-753-2020>.
- Shahid, M. & Rahman, K. U. 2020 Identifying the annual and seasonal trends of hydrological and climatic variables in the Indus Basin Pakistan. *Asia-Pacific Journal of Atmospheric Sciences*. <https://doi.org/10.1007/s13143-020-00194-2>.
- Shamshirband, S., Hashemi, S., Salimi, H., Samadianfar, S., Asadi, E., Shadkani, S. & Chau, K. W. 2020 Predicting Standardized Streamflow index for hydrological drought using machine learning models. *Engineering Applications of Computational Fluid Mechanics* **14** (1), 339–350. <https://doi.org/10.1080/19942060.2020.1715844>.
- Shawul, A. A. & Chakma, S. 2020 Suitability of global precipitation estimates for hydrologic prediction in the main watersheds of Upper Awash basin. *Environmental Earth Sciences* **79** (2), 1–18. <https://doi.org/10.1007/s12665-019-8801-3>.
- Stagge, J. H., Tallaksen, L. M., Gudmundsson, L., Van Loon, A. F. & Stahl, K. 2015 Candidate distributions for climatological drought indices (SPI and SPEI). *International Journal of Climatology* **35** (13), 4027–4040. <https://doi.org/10.1002/joc.4267>.
- Stampfli, A., Bloor, J. M. G., Fischer, M. & Zeiter, M. 2018 High land-use intensity exacerbates shifts in grassland vegetation composition after severe experimental drought. *Global Change Biology* **24** (5), 2021–2034. <https://doi.org/10.1111/gcb.14046>.
- Sun, Q., Miao, C., Duan, Q., Ashouri, H., Sorooshian, S. & Hsu, K. L. 2018 A review of global precipitation data sets: data sources, estimation, and intercomparisons. *Reviews of Geophysics* **56** (1), 79–107. <https://doi.org/10.1002/2017RG000574>.
- Tirivarombo, S., Osupile, D. & Eliasson, P. 2018 Drought monitoring and analysis: Standardised Precipitation Evapotranspiration Index (SPEI) and Standardised Precipitation Index (SPI). *Physics and Chemistry of the Earth* **106**, 1–10. <https://doi.org/10.1016/j.pce.2018.07.001>.
- Umiahi, T., Suroso & Ardiansyah. 2019 Spatial analysis and monitoring of drought using Standardized Precipitation

- Index in East Java. *Journal of Physics: Conference Series* **1367** (1), 012088.
- Wang, H. & Asefa, T. 2019 [Drought monitoring, mitigation, and adaptation](#). In: *Extreme Hydrology and Climate Variability: Monitoring, Modelling, Adaptation and Mitigation*. <https://doi.org/10.1016/B978-0-12-815998-9.00036-1>.
- Wang, L., Yu, H., Yang, M., Yang, R., Gao, R. & Wang, Y. 2019 [A drought index: the standardized precipitation evapotranspiration runoff index](#). *Journal of Hydrology* **571**, 651–668. <https://doi.org/10.1016/j.jhydrol.2019.02.023>.
- Wijekularathna, D. K., Manage, A. B. W. & Scariano, S. M. 2019 [Power analysis of several normality tests: a Monte Carlo simulation study](#). *Communications in Statistics: Simulation and Computation*, 1–17. <https://doi.org/10.1080/03610918.2019.1658780>.
- World Bank 2019 *Indonesia Economic Quarterly, December 2019: Investing in People*. World Bank, Washington, DC.
- World Meteorological Organization 2012 *Standardized Precipitation Index User Guide* (M. Svoboda, M. Hayes & D. Wood, eds.). World Meteorological Organization, Geneva, Switzerland.
- Zhang, Y., Wang, J., Shen, Z. & Xie, X. 2019 [Evolution characteristics of seasonal drought in hunan based on the standardized precipitation index \(SPI\)](#). *Geoscience and Remote Sensing* **2**, 56–64. <https://doi.org/10.23977/geors.2019.21004>.

First received 19 January 2021; accepted in revised form 29 April 2021. Available online 18 May 2021

# Drought detection in Java Island based on Standardized Precipitation and Evapotranspiration Index (SPEI)

## ORIGINALITY REPORT

15%

SIMILARITY INDEX

10%

INTERNET SOURCES

14%

PUBLICATIONS

4%

STUDENT PAPERS

## PRIMARY SOURCES

- |   |  |    |
|---|--|----|
| 1 | Submitted to University of South Australia<br>Student Paper  | 2% |
| 2 | Alexis Kirsten Cooley, Heejun Chang.<br>"Detecting change in precipitation indices using observed (1977–2016) and modeled future climate data in Portland, Oregon, USA",<br>Journal of Water and Climate Change, 2021<br>Publication | 2% |
| 3 | Lele Zhang, Liming Gao. "Drought and Wetness Variability and the Respective Contribution of Temperature and Precipitation in the Qinghai-Tibetan Plateau",<br>Advances in Meteorology, 2021<br>Publication                           | 1% |
| 4 | Iwaponline.Com<br>Internet Source  | 1% |
| 5 | James H. Stagge, Lena M. Tallaksen, Lukas Gudmundsson, Anne F. Van Loon, Kerstin Stahl. "Candidate Distributions for   | 1% |

# Climatological Drought Indices ( and ) ", International Journal of Climatology, 2015

Publication

---

6	<a href="http://www.tandfonline.com">www.tandfonline.com</a> Internet Source	<1 %
7	<a href="http://esdd.copernicus.org">esdd.copernicus.org</a> Internet Source	<1 %
8	<a href="http://link.springer.com">link.springer.com</a> Internet Source	<1 %
9	<a href="http://www.mdpi.com">www.mdpi.com</a> Internet Source	<1 %
10	N T Monish, S Rehana. "Suitability of distributions for standard precipitation and evapotranspiration index over meteorologically homogeneous zones of India", Journal of Earth System Science, 2019 Publication	<1 %
11	S. Tirivarombo, D. Osupile, P. Eliasson. "Drought monitoring and analysis: Standardised Precipitation Evapotranspiration Index (SPEI) and Standardised Precipitation Index (SPI)", Physics and Chemistry of the Earth, Parts A/B/C, 2018 Publication	<1 %
12	Zhifang Pei, Shibo Fang, Lei Wang, Wunian Yang. "Comparative Analysis of Drought Indicated by the SPI and SPEI at Various	<1 %

---

# Timescales in Inner Mongolia, China", Water, 2020

Publication

13

Tri Umiati, Suroso, Ardiansyah. "Spatial analysis and monitoring of drought using Standardized Precipitation Index in East Java", Journal of Physics: Conference Series, 2019

Publication

<1 %

14

Monica Ionita, Viorica Nagavciuc. "Changes in drought features at the European level over the last 120 years", Natural Hazards and Earth System Sciences, 2021

Publication

<1 %

15

[jkscoe.or.kr](http://jkscoe.or.kr)

Internet Source

<1 %

16

Zhang, Baoqing, Zikui Wang, and Guan Chen. "A sensitivity study of applying a two-source potential evapotranspiration model in the Standardized Precipitation Evapotranspiration Index for drought monitoring : Two-Source PET model is used and evaluated in calculating the SPEI", Land Degradation and Development, 2016.

Publication

<1 %

17

[munin.uit.no](http://munin.uit.no)

Internet Source

<1 %

18

[CLIMATEDATAGUIDE.UCAR.EDU](http://CLIMATEDATAGUIDE.UCAR.EDU)

Internet Source

<1 %

19

Mishra, A.K.. "Drought forecasting using feed-forward recursive neural network", Ecological Modelling, 20060915

Publication

<1 %

20

[journals.plos.org](http://journals.plos.org)

Internet Source

<1 %

21

[www.gssrr.org](http://www.gssrr.org)

Internet Source

<1 %

22

[gmd.copernicus.org](http://gmd.copernicus.org)

Internet Source

<1 %

23

[www.nature.com](http://www.nature.com)

Internet Source

<1 %

24

[www.unccd.int](http://www.unccd.int)

Internet Source

<1 %

25

Potop, V.. "Drought evolution at various time scales in the lowland regions and their impact on vegetable crops in the Czech Republic", Agricultural and Forest Meteorology, 20120415

Publication

<1 %

26

[journal.ugm.ac.id](http://journal.ugm.ac.id)

Internet Source

<1 %

27	Mohammad Ilyas Abro, Ehsan Elahi, Ram Chand, Dehua Zhu et al. "Estimation of a trend of meteorological and hydrological drought over Qinhuai River Basin", Theoretical and Applied Climatology, 2021 Publication	<1 %
28	Submitted to University of Brighton Student Paper	<1 %
29	ephyslab.uvigo.es Internet Source	<1 %
30	icdc.cen.uni-hamburg.de Internet Source	<1 %
31	Qiaohong Sun, Chiyuan Miao, Qingyun Duan, Hamed Ashouri, Soroosh Sorooshian, Kuo-Lin Hsu. "A Review of Global Precipitation Data Sets: Data Sources, Estimation, and Intercomparisons", Reviews of Geophysics, 2018 Publication	<1 %
32	Yue Qin, Dawen Yang, Huimin Lei, Kai Xu, Xiangyu Xu. "Comparative analysis of drought based on precipitation and soil moisture indices in Haihe basin of North China during the period of 1960–2010", Journal of Hydrology, 2015 Publication	<1 %

33	Amare Sisay Tefera, J. O. Ayoade, N. J. Bello. "Comparative analyses of SPI and SPEI as drought assessment tools in Tigray Region, Northern Ethiopia", SN Applied Sciences, 2019 Publication	<1 %
34	Ankit Shekhar, Charles A. Shapiro. "What do meteorological indices tell us about a long-term tillage study?", Soil and Tillage Research, 2019 Publication	<1 %
35	ebin.pub Internet Source	<1 %
36	S. Bachmair, C. Svensson, J. Hannaford, L. J. Barker, K. Stahl. "A quantitative analysis to objectively appraise drought indicators and model drought impacts", Hydrology and Earth System Sciences Discussions, 2015 Publication	<1 %
37	Univendspace.univen.ac.za Internet Source	<1 %
38	qdoc.tips Internet Source	<1 %
39	N L Adhyani, T June, A Sopaheluwakan. "Exposure to Drought: Duration, Severity and Intensity (Java, Bali and Nusa Tenggara)", IOP Conference Series: Earth and Environmental Science, 2017	<1 %

40

Peyman Mahmoudi, Alireza Ghaemi, Allahbakhsh Rigi, Seyed Mahdi Amir Jahanshahi. "Recommendations for modifying the Standardized Precipitation Index (SPI) for Drought Monitoring in Arid and Semi-arid Regions", Water Resources Management, 2021

Publication

<1 %

41

Shanhu Jiang, Linyong Wei, Liliang Ren, Chong-Yu Xu, Feng Zhong, Menghao Wang, Linqi Zhang, Fei Yuan, Yi Liu. "Utility of integrated IMERG precipitation and GLEAM potential evapotranspiration products for drought monitoring over mainland China", Atmospheric Research, 2021

Publication

<1 %

42

Wenhan Lv, Chuanhao Wu, Pat J. - F. Yeh, Bill X. Hu. " Spatio - temporal variability of dryness and wetness based on indices and its relation to the ", International Journal of Climatology, 2021

Publication

<1 %

43

repositorio.ufrn.br  
Internet Source

<1 %

44

statistik.econ.kit.edu  
Internet Source

<1 %

45	Baraniko Namanoku. "Drought and its social, environmental and economic negative impact in Kiribati with a specific case study of South Tarawa", Repositório Aberto da Universidade do Porto, 2014. Publication	<1 %
46	Faradiba. "Analysis of Intensity, Duration, and Frequency Rain Daily of Java Island Using Mononobe Method", Journal of Physics: Conference Series, 2021 Publication	<1 %
47	Priyanko Das, Zhenke Zhang, Hang Ren. "Evaluating the accuracy of two satellite-based Quantitative Precipitation Estimation products and their application for meteorological drought monitoring over the Lake Victoria Basin, East Africa", Geo-spatial Information Science, 2022 Publication	<1 %
48	<a href="https://iopscience.iop.org">iopscience.iop.org</a> Internet Source	<1 %
49	<a href="https://ueaeprints.uea.ac.uk">ueaeprints.uea.ac.uk</a> Internet Source	<1 %
50	Jaewon Jang, Yesol Kang, Kyunghoon Jang, Suhun Kim, Sang-Soo Chee, In S. Kim. "Ti3C2TX-Ethylenediamine Nanofiltration	<1 %

# Membrane for High Rejection of Heavy Metals", Chemical Engineering Journal, 2022

Publication

---

51 Mokhtar Karami, Mehdi Asadi. "Investigating the inter-annual precipitation changes of Iran", Journal of Water and Climate Change, 2020

Publication

---

52 Sylus Kipngeno Musei, Justine Muhoro Nyaga, Abdi Zeila Dubow. "SPEI-based spatial and temporal evaluation of drought in Somalia", Journal of Arid Environments, 2020

Publication

---

53 Yaojie Liu, Cuihai You, Yongguang Zhang, Shiping Chen, Zhaoying Zhang, Ji Li, Yunfei Wu. "Resistance and resilience of grasslands to drought detected by SIF in inner Mongolia, China", Agricultural and Forest Meteorology, 2021

Publication

---

54 [core.ac.uk](https://core.ac.uk)

Internet Source

---

55 [digitalcommons.unl.edu](https://digitalcommons.unl.edu)

Internet Source

---

56 [seekingalpha.com](https://seekingalpha.com)

Internet Source

---

57

A Subiyanto, IDK K Widana, A M Julius.  
"Resilience: A new concepts in dealing with  
hydro-meteorological disaster and it's  
application at the provincial level in  
Indonesia", IOP Conference Series: Earth and  
Environmental Science, 2021

Publication

&lt;1 %

58

Ali Danandeh Mehr, Ali Unal Sorman, Ercan  
Kahya, Mahdi Hesami Afshar. "Climate change  
impacts on meteorological drought using SPI  
and SPEI: case study of Ankara, Turkey",  
Hydrological Sciences Journal, 2019

Publication

&lt;1 %

59

Bachmair, S., I. Kohn, and K. Stahl. "Exploring  
the link between drought indicators and  
impacts", Natural Hazards and Earth System  
Science, 2015.

Publication

&lt;1 %

60

Brecht Martens, Richard de Jeu, Niko  
Verhoest, Hanneke Schuurmans, Jonne Kleijer,  
Diego Miralles. "Towards Estimating Land  
Evaporation at Field Scales Using GLEAM",  
Remote Sensing, 2018

Publication

&lt;1 %

61

Fernanda Rodrigues Fernandes, Leonardo  
Dominici Cruz, Eduardo Guimarães Martins,  
Sérgio Furtado dos Reis. " Growth and home  
range size of the gracile mouse opossum

&lt;1 %

(Marsupialia: Didelphidae) in Brazilian cerrado  
", Journal of Tropical Ecology, 2010

Publication

62

Gebremedhin Gebremeskel Haile, Qihong Tang, Seyed - Mohammad Hosseini - Moghari, Xingcai Liu et al. "Projected Impacts of Climate Change on Drought Patterns Over East Africa", Earth's Future, 2020

Publication

<1 %

63

Huaijun Wang, Yingping Pan, Yaning Chen. "Comparison of three drought indices and their evolutionary characteristics in the arid region of northwestern China", Atmospheric Science Letters, 2017

Publication

<1 %

64

Huanyu Wu, Yong Zou, Lincoln M. Alves, Elbert E. N. Macau, Gilvan Sampaio, Jose A. Marengo. "Uncovering episodic influence of oceans on extreme drought events in Northeast Brazil by ordinal partition network approaches", Chaos: An Interdisciplinary Journal of Nonlinear Science, 2020

Publication

<1 %

65

Jimmy Byakatonda, Geoffrey Openy, Jotham Ivan Sempewo, Dominic Banaga Mucunguzi. "Over a century evidence of historical and recent dryness/wetness in sub - humid areas:

<1 %

# A Uganda, East African case", Meteorological Applications, 2021

Publication

66

Joseph Mukasa, Lydia Olaka, Mohammed Yahya Said. "Drought and households' adaptive capacity to water scarcity in Kasali, Uganda", Journal of Water and Climate Change, 2020

Publication

<1 %

67

Paulo, A.A.. "Drought class transition analysis through Markov and Loglinear models, an approach to early warning", Agricultural Water Management, 20050822

Publication

<1 %

68

Tayyebbeh Mesbahzadeh, Maryam Mirakbari, Mohsen Mohseni Saravi, Farshad Soleimani Sardoo, Mario M. Miglietta. "Meteorological drought analysis using copula theory and drought indicators under climate change scenarios (RCP)", Meteorological Applications, 2019

Publication

<1 %

69

[cp.copernicus.org](http://cp.copernicus.org)

Internet Source

<1 %

70

[etd.aau.edu.et](http://etd.aau.edu.et)

Internet Source

<1 %

71

[ir.lib.uth.gr](http://ir.lib.uth.gr)

Internet Source

<1 %

72

[journals.ametsoc.org](http://journals.ametsoc.org)

Internet Source

<1 %

73

[padresrundown.blogspot.com](http://padresrundown.blogspot.com)

Internet Source

<1 %

74

Brecht Martens, Diego G. Miralles, Hans Lievens, Robin van der Schalie et al.

"GLEAM v3: satellite-based land evaporation and root-zone soil moisture", Geoscientific Model Development, 2017

Publication

<1 %

75

Laura Melo Vieira Soares. "Synergistic interaction among reservoirs along a cascade system and their response to the ongoing anthropogenic and climatic pressures: evidence from deterministic hydrodynamic-biogeochemical modelling", Universidade de Sao Paulo, Agencia USP de Gestao da Informacao Academica (AGUIA), 2021

Publication

<1 %

76

Xue Li, Jian Sha, Zhong-Liang Wang. "Comparison of drought indices in the analysis of spatial and temporal changes of climatic drought events in a basin", Environmental Science and Pollution Research, 2019

Publication

<1 %

---

77

Gabriel Constantino Blain, Ana Maria H. de Avila, Vânia Rosa Pereira. "Using the normality assumption to calculate probability-based standardized drought indices: selection criteria with emphases on typical events", International Journal of Climatology, 2018

Publication

<1 %

---

78

Philip G. Oguntunde, Gunnar Lischeid, Babatunde J. Abiodun, Ottfried Dietrich. "Analysis of long-term dry and wet conditions over Nigeria", International Journal of Climatology, 2017

Publication

<1 %

---

Exclude quotes      On

Exclude matches      Off

Exclude bibliography      On